2007

Theoretical Study of the Pyrolysis of Methyltrichlorosilane in the Gas Phase. 2. Reaction Paths and Transition States

Yingbin Ge
Iowa State University

Mark S. Gordon
Iowa State University, mgordon@iastate.edu

Francine Battaglia
Iowa State University

See next page for additional authors

Theoretical Study of the Pyrolysis of Methyltrichlorosilane in the Gas Phase. 2. Reaction Paths and Transition States

Abstract
The kinetics for the previously proposed 114-reaction mechanism for the chemical vapor deposition (CVD) process that leads from methyltrichlorosilane (MTS) to silicon carbide (SiC) are examined. Among the 114 reactions, 41 are predicted to proceed with no intervening barrier. For the remaining 73 reactions, transition states and their corresponding barrier heights have been explored using second-order perturbation theory (MP2) with the aug-cc-pVDZ basis set. Final energies for the reaction barriers were obtained using both MP2 with the aug-cc-pVTZ basis set and coupled cluster theory (CCSD(T)) with the aug-cc-pVDZ basis set. CCSD(T)/aug-cc-pVTZ energies were estimated by assuming additivity of basis set and correlation effects. Partition functions for the computation of thermodynamic properties of the transition states were calculated with MP2/aug-cc-pVDZ. Forward and reverse Gibbs free energy barriers were obtained at 11 temperatures ranging from 0 to 2000 K. Important reaction pathways are illustrated at 0 and 1400 K.

Disciplines
Biological Engineering | Chemical Engineering | Chemistry | Mechanical Engineering

Comments
This article is from *Journal of Physical Chemistry A* 111 (2007): 1475-1486, doi: 10.1021/jp065455a. Posted with permission.

Authors
Yingbin Ge, Mark S. Gordon, Francine Battaglia, and Rodney O. Fox

Theoretical Study of the Pyrolysis of Methyltrichlorosilane in the Gas Phase. 2. Reaction Paths and Transition States

Yingbin Ge and Mark S. Gordon*

Department of Chemistry, Iowa State University, Ames, Iowa 50011

Francine Battaglia

Department of Mechanical Engineering, Iowa State University, Ames, Iowa 50011

Rodney O. Fox

Department of Chemical and Biological Engineering, Iowa State University, Ames, Iowa 50011

Received: August 23, 2006; In Final Form: November 27, 2006

The kinetics for the previously proposed 114-reaction mechanism for the chemical vapor deposition (CVD) process that leads from methyltrichlorosilane (MTS) to silicon carbide (SiC) are examined. Among the 114 reactions, 41 are predicted to proceed with no intervening barrier. For the remaining 73 reactions, transition states and their corresponding barrier heights have been explored using second-order perturbation theory (MP2) with the aug-cc-pVDZ basis set. Final energies for the reaction barriers were obtained using both MP2 with the aug-cc-pVTZ basis set and coupled cluster theory (CCSD(T)) with the aug-cc-pVDZ basis set. CCSD(T)/aug-cc-pVTZ energies were estimated by assuming additivity of basis set and correlation effects. Partition functions for the computation of thermodynamic properties of the transition states were calculated with MP2/aug-cc-pVDZ. Forward and reverse Gibbs free energy barriers were obtained at 11 temperatures ranging from 0 to 2000 K. Important reaction pathways are illustrated at 0 and 1400 K.

I. Introduction

In the previous paper,[1] a mechanism consisting of 114 reactions was proposed to account for the production and consumption of the various gas-phase species in the chemical vapor deposition of silicon carbide, starting from methyltrichlorosilane (MTS). In the present work, the transition states and associated barrier heights, as well as minimum energy reaction paths, are considered. Some of the reactions in this network have been studied previously. Gordon et al. studied the thermal decomposition pathways of ethane using the MP4/6-311G(d,p)//HF/6-31G(d) method[2] and concluded that the cleavage of the C−C bond was the most kinetically favored decomposition reaction path with an 85 kcal/mol energy barrier at 0 K. The direct 1,2-elimination of hydrogen has a much larger 130 kcal/mol barrier, even though it is thermodynamically favored. Jensen et al. studied the $C_2H_4 \rightarrow C_2H_2 + H_2$ reaction at the MP4/6-311+G(d,p)//MP2/6-31G(d) level of theory.[3] Two pathways were proposed. One involves the formation of ethylidene (CH_3-CH) and the other involves the formation of vinylidene (CH_2C) as an intermediate. A direct 1,2-elimination pathway of H_2 from ethylene was not found. Allendorf et al. studied various reaction pathways related to the decomposition of MTS using MP4/6-31G(d,p)//HF/6-31G(d) with empirical bond additivity corrections (BAC).[4,5] Their results suggest that Si−C bond cleavage, C−H bond cleavage, and 1,2-elimination of HCl are the predominant decomposition pathways of MTS at 800−1500 K. However, consecutive reactions after MTS decomposition are not discussed in their papers.

Diau et al. studied the $CH_3 + C_2H_2$ reactions theoretically.[6] They found that $CH_3 + C_2H_2 \rightarrow CH_3CH{=}CH$ is the primary reaction at <1300 K. At temperatures >1400 K and atmospheric pressure, $CH_3 + C_2H_2 \rightarrow CH_3CCH + H$ becomes the major reaction pathway. Hase et al. calculated the energy barrier for the $C_2H_4 + H \rightarrow C_2H_5$ reaction using the UMP2, QCISD, and MRCI methods with various basis sets.[7] They also calculated the reaction rate constants, which agreed well with experimental values.[8−12]

Liu et al. studied $C_2H_3 + CH_4 \rightarrow C_2H_4 + CH_3$ and $C_2H_3 + C_2H_6 \rightarrow C_2H_4 + C_2H_5$ using the G2//MP2 and G2//QCISD methods.[13] They obtained the rate constants using transition state theory (TST) and canonical variational transition state theory (CVT) and concluded that $C_2H_3 + C_2H_6 \rightarrow C_2H_4 + C_2H_5$ was faster than $C_2H_3 + CH_4 \rightarrow C_2H_4 + CH_3$ at 200−3000 K. Wu et al. applied the CCSD(T) method to investigate the potential energy surface of $H + CH_4 \rightarrow H_2 + CH_3$ and predicted its rate constant with an accuracy comparable to that of experiments.[14] They also found that rate constants predicted by transition state theory are reasonably accurate at temperatures above 500 K. However, the effect of tunneling becomes nontrivial at temperatures below 400 K.

Wittbrodt and Schlegel studied the thermal decomposition of dichlorosilane and obtained estimated QCISD(T)/6-311++G-(3df,3pd) energies for reactants, products, and transition states by assuming additivity of basis set and correlation corrections.[15] The preferred decomposition pathway was found to be $SiH_2Cl_2 \rightarrow SiHCl + HCl$ with a 70.8 kcal/mol barrier at 298 K, 1.9 kcal/mol lower than that of $SiH_2Cl_2 \rightarrow SiCl_2 + H_2$. Walch et al. investigated the thermal decomposition pathways and rate constants for silane, chlorosilane, dichlorosilane, and trichlo-

* Corresponding author. Tel: 515-294-0452. Fax: 515-294-0105. E-mail: mark@si.fi.ameslab.gov.

10.1021/jp065455a CCC: $37.00
Published on Web 02/03/2007

rosilane, using CCSD(T) energies extrapolated to the complete basis set limit at CASSCF/cc-pVDZ geometries.[16] They also studied reactions of $SiCl_2$ and SiHCl with H and Cl atoms using the same method.[17] Their classical barrier heights (kcal/mol) related to this paper are $SiH_2Cl_2 \rightarrow SiHCl + HCl$ (74.8), $SiH_2Cl_2 \rightarrow SiCl_2 + H_2$ (77.2), $SiHCl_3 \rightarrow SiCl_2 + HCl$ (72.7), $SiHCl + H \rightarrow SiH + HCl$ (13.5), $SiHCl + Cl \rightarrow SiH + Cl_2$ (2.0), and $SiCl + HCl \rightarrow SiHCl_2$ (32.4). The $SiHCl + H \rightarrow SiCl + H_2$ and $SiHCl + Cl \rightarrow SiCl + HCl$ reactions are predicted to be barrierless.

Despite several previous studies of C−H−Si−Cl, C−H, and H−Si−Cl systems, the present work is the first electronic structure theory study that thoroughly investigates all reactions during and after the decomposition of MTS in the gas-phase that may have a significant effect on the gas-phase composition during the SiC CVD process and/or on the concentration of the major species that account for the deposition and growth of silicon carbide.

II. Computational Details

Geometries, harmonic vibrational frequencies, and zero point energies of all transition state structures have been obtained at the unrestricted MP2 (UMP2)[18] level of theory with the aug-cc-pVDZ basis set.[19,20] Transition state structures have one imaginary frequency, determined by computing and diagonalizing the matrix of energy second derivatives (Hessian). Minimum energy path (MEP) calculations were performed to confirm that the located transition state structures connect the expected reactants and products. The partition functions were calculated within the harmonic oscillator/rigid rotor approximation, at temperatures ranging from 0 to 2000 K. Single-point energies were obtained at these geometries using MP2/aug-cc-pVTZ[19,20] and CCSD(T)/aug-cc-pVDZ. CCSD(T)/aug-cc-pVTZ single point energies were estimated by assuming additivity of basis set and correlation corrections:

$$E_{\mathrm{CCSD(T)/aug-cc-pVTZ}} \approx E_{\mathrm{CCSD(T)/aug-cc-pVDZ}} + (E_{\mathrm{MP2/aug-cc-pVTZ}} - E_{\mathrm{MP2/aug-cc-pVDZ}}) \quad (1)$$

All of the MP2 calculations were done with the GAMESS suite of codes.[21] CCSD(T)/aug-cc-pVTZ singlet point calculations were performed using the ACES package.[22]

Structures, vibrational frequencies, and minimum energy paths were visualized with the aid of MacMolPlt.[23]

III. Results and Discussion

In the preceding paper, a 114-reaction mechanism was proposed to account for the gas-phase chemistry of SiC CVD started from MTS and H_2 as feeding gas.[1] In the present work, 41 reactions have been determined to have no well-defined transition state (TS) by the following means. First, bond-breaking reactions without significant reconstruction of electronic structure are assumed to have no well-defined transition state. For example: $CH_3SiCl_3 \rightarrow CH_3 + SiCl_3$ simply breaks a C−Si bond to form two radical fragments. Second, rate expressions have been obtained from others previous research. Constant reaction rate expression within a wide temperature range often suggest the reaction has no well-defined transition state, such as $^3CH_2 + CH_3 \rightarrow C_2H_4 + H$[24] and $^3CH_2 + {}^3CH_2 \rightarrow C_2H_2 + H_2$[24]. Third, constrained geometry optimizations were performed to obtain approximate reaction paths that ensure that a reaction has no energy barrier. This approach provides indirect evidence that no transition state is present (for example, $SiCl_3 \rightarrow SiCl_2 + Cl$). In the following discussion, these reactions will be referred to as having no transition state.

Figure 1 illustrates key structural information in the TS region for the 73 transition states that were found. Each transition state is labeled with "TS" followed by an arbitrarily assigned number. The corresponding reactions can be found in the first columns of Tables 1−3, which are labeled in a consistent way with the transition states in Figure 1. MP2 and CCSD(T) energies and zero point energies (ZPE) of these transition states are tabulated in the Supporting Information.

Tables 1−3 list forward and reverse enthalpies, entropies, and Gibbs free energies of activation, respectively, for the 73 reactions at 0−2000 K. The harmonic oscillator/rigid rotor approximation has been employed to construct the appropriate partition functions. Classical energy barriers have been obtained by calculating the estimated CCSD(T)/aug-cc-pVTZ energy difference between transition states and reactants or products at MP2/aug-cc-pVDZ geometries. Enthalpies of activation have been obtained by adding MP2/aug-cc-pVDZ ZPE and thermodynamic corrections at various temperatures to the classical barriers. Negative enthalpies of activation most likely occur due to their computation using single point CCSD(T) energies at MP2 structures. This could mean either that the TS location shifts at the higher level of theory or that the TS actually disappears at the higher level of theory. For very small classical barriers, it is also possible that the addition of ZPE is sufficient to reduce the enthalpy of activation to zero.

Table 2 shows that a transition state often has a higher entropy than the reactant in unimolecular reactions but a lower entropy than reactants in bimolecular reactions. This is expected, because a transition state usually has a looser structure than a unimolecular reactant but tighter structure than the two bimolecular reactants. The Gibbs free energies of activation in Table 3 may be useful for future rate constant calculations using transition state theory.

Figures 2−6 illustrate five important potential energy surfaces. Gibbs free energies of minima and transition states are obtained in the following way: classical energies are estimated CCSD(T)/aug-cc-pVTZ energies (calculated using eq 1) at MP2/aug-cc-pVDZ structures; ZPE and thermodynamic properties are calculated with MP2/aug-cc-pVDZ. Relative Gibbs free energies are given at 0 and 1400 K, because 1400 K is a typical SiC CVD temperature. The species with the lowest Gibbs free energy at 0 K is selected as the reference when relative Gibbs free energies are calculated. Note that Gibbs free energy barriers of the reactions without a transition state presented in this paper are assumed to be equal to the absolute values of the corresponding reaction free energies. More accurate free energies of activation of the reactions without TS will be obtained in a subsequent work by a means of free energy profiling along the minimal energy path. These five reactions are discussed in the following sub-sections.

A. Unimolecular Decomposition of CH_3SiCl_3. Eight unimolecular decomposition pathways are illustrated in Figure 2. Three are simple bond-cleavage reactions with no transition states: $CH_3SiCl_3 \rightarrow CH_3 + SiCl_3$, $CH_3SiCl_3 \rightarrow CH_2SiCl_3 + H$, and $CH_3SiCl_3 \rightarrow CH_3SiCl_2 + Cl$. The forward Gibbs free energies of activation for these three reactions (which correspond to the net reaction endothermicities) are 91.6, 101.1, and 108.4 kcal/mol at 0 K, respectively. However, at 1400 K, these free energies are reduced to 38.1, 51.4, and 61.1 kcal/mol, respectively. This significant decrease at 1400 K is mainly due to the entropy increase when CH_3SiCl_3 dissociates.

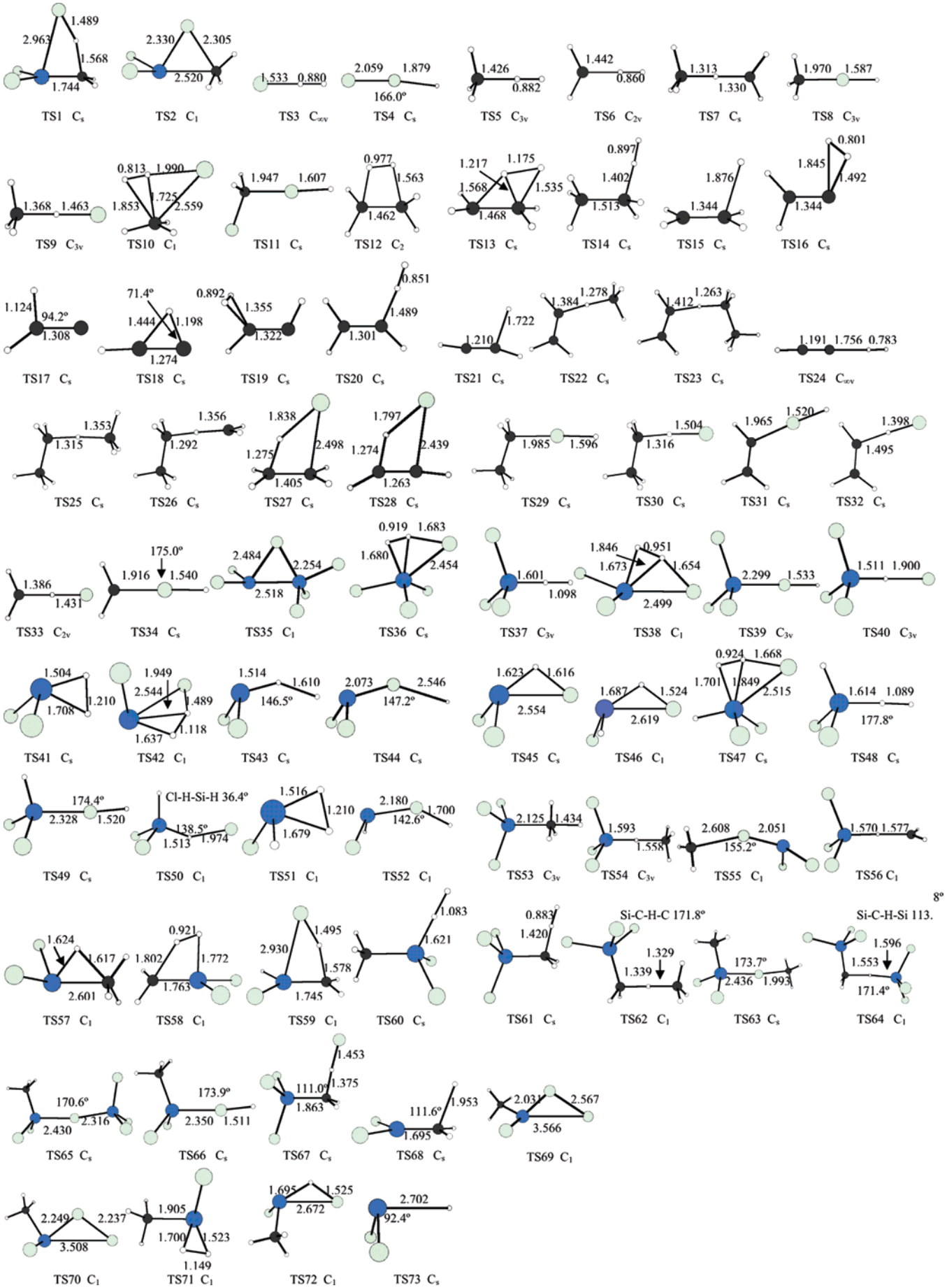

Figure 1. MP2/aug-cc-PVDZ transition state structures. Bond lengths in angstroms; bond angles and dihedral angles in degrees. The corresponding reactions can be found in the first columns of Tables 1−3.

TABLE 1: Forward (Upper Entry) and Reverse (Lower Entry) Activation Enthalpies (kcal/mol) at Various Temperatures Ranging from 0 to 2000 K[a]

reaction	0 K	298.15 K	400 K	600 K	800 K	1000 K	1200 K	1400 K	1600 K	1800 K	2000 K
TS1. $CH_3SiCl_3 \rightarrow CH_2SiCl_2 + HCl$	81.0	81.1	81.1	81.2	81.3	81.3	81.2	81.1	80.9	80.7	80.5
	2.2	1.2	1.2	1.3	1.5	1.9	2.2	2.5	2.9	3.2	3.5
TS2. $CH_3SiCl_3 \rightarrow CH_3Cl + SiCl_2$	109.0	109.3	109.2	109.1	108.8	108.5	108.1	107.7	107.3	106.9	106.5
	36.4	36.2	36.5	37.2	37.7	38.2	38.7	39.1	39.5	40.0	40.4
TS3. $Cl + H_2 \rightarrow HCl + H$	5.4	4.2	4.0	3.7	3.6	3.6	3.6	3.6	3.6	3.5	3.5
	3.8	2.7	2.5	2.2	2.1	2.0	1.9	1.8	1.7	1.6	1.4
TS4. $Cl + HCl \rightarrow Cl_2 + H$	47.8	47.1	47.0	46.9	46.8	46.7	46.6	46.4	46.2	45.9	45.7
	0.4	−0.4	−0.6	−1.1	−1.5	−1.9	−2.3	−2.7	−3.1	−3.5	−3.9
TS5. $CH_3 + H_2 \rightarrow CH_4 + H$	13.6	11.7	11.3	10.8	10.7	10.8	11.0	11.2	11.5	11.8	12.1
	13.1	11.9	11.8	11.7	11.7	11.7	11.7	11.6	11.6	11.5	11.4
TS6. $CH_3 + H \rightarrow {}^3CH_2 + H_2$	14.5	13.3	13.1	12.9	12.7	12.6	12.6	12.5	12.4	12.3	12.2
	9.5	7.8	7.5	7.3	7.3	7.5	7.7	8.0	8.3	8.6	8.9
TS7. $CH_3 + CH_3 \rightarrow {}^3CH_2 + CH_4$	16.8	15.5	15.4	15.6	16.0	16.5	17.1	17.6	18.2	18.7	19.2
	11.3	10.3	10.4	10.9	11.6	12.3	12.9	13.5	14.1	14.7	15.2
TS8. $CH_3 + HCl \rightarrow CH_3Cl + H$	30.6	29.2	29.0	28.9	29.1	29.3	29.7	30.0	30.3	30.6	30.9
	10.1	9.3	9.2	9.1	9.0	8.9	8.7	8.5	8.4	8.2	8.0
TS9. $CH_3 + HCl \rightarrow CH_4 + Cl$	2.3	0.7	0.5	0.4	0.6	0.9	1.2	1.5	1.8	2.1	2.4
	3.3	2.5	2.6	2.9	3.2	3.4	3.6	3.7	3.7	3.8	3.7
TS10. $CH_3Cl + H_2 \rightarrow CH_4 + HCl$	86.9	85.8	85.8	85.8	86.0	86.2	86.4	86.6	86.8	87.1	87.3
	107.0	105.9	106.0	106.5	107.0	107.6	108.0	108.4	108.8	109.1	109.4
TS11. $CH_2Cl + HCl \rightarrow CH_2Cl_2 + H$	33.2	31.9	31.8	31.8	32.1	32.4	32.7	33.1	33.4	33.7	34.0
	9.2	8.3	8.2	8.0	7.9	7.7	7.5	7.4	7.2	7.0	6.8
TS12. $C_2H_6 \rightarrow C_2H_4 + H_2$	122.9	122.9	122.9	123.0	123.1	123.2	123.2	123.2	123.1	123.0	122.8
	91.6	89.8	89.3	88.8	88.5	88.6	88.7	88.9	89.2	89.5	89.7
TS13. $C_2H_6(e) \rightarrow C_2H_4 + H_2$	113.5	113.7	114.0	114.7	115.3	115.8	116.2	116.6	116.9	117.1	117.3
	84.7	82.9	82.5	82.1	81.9	82.0	82.1	82.3	82.6	82.8	83.1
TS14. $C_2H_6 + H \rightarrow C_2H_5 + H_2$	10.2	9.2	9.0	8.9	8.9	8.9	8.9	8.9	8.8	8.7	8.6
	14.0	12.1	11.7	11.3	11.2	11.3	11.5	11.7	12.0	12.3	12.6
TS15. $C_2H_5 \rightarrow C_2H_4 + H$	38.9	38.7	38.6	38.6	38.6	38.5	38.4	38.2	38.0	37.7	37.4
	3.9	2.7	2.4	2.1	1.8	1.5	1.3	1.0	0.8	0.6	0.4
TS16. $C_2H_4 \rightarrow CH_2C + H_2$	92.6	93.0	93.3	93.8	94.2	94.4	94.4	94.4	94.3	94.1	93.9
	10.5	8.5	8.2	7.8	7.6	7.6	7.7	7.8	8.0	8.2	8.3
TS17. $CH_2C \rightarrow HCHC$	0.5	0.3	0.1	−0.3	−0.6	−1.0	−1.4	−1.7	−2.1	−2.5	−2.9
	−0.8	−1.0	−1.1	−1.5	−1.8	−2.3	−2.7	−3.1	−3.6	−4.0	−4.4
TS18. $HCHC \rightarrow C_2H_2$	0.1	0.0	−0.1	−0.4	−0.7	−1.1	−1.4	−1.8	−2.2	−2.6	−3.0
	43.6	43.5	43.3	42.8	42.3	41.8	41.3	40.8	40.3	39.7	39.2
TS19. $CH_3CH(s) \rightarrow C_2H_2 + H_2$	33.2	33.4	33.6	33.9	34.3	34.5	34.8	35.0	35.1	35.3	35.4
	66.4	64.4	63.7	62.8	62.2	61.9	61.7	61.7	61.6	61.7	61.7
TS20. $C_2H_4 + H \rightarrow C_2H_3 + H_2$	17.1	16.1	16.0	15.8	15.7	15.5	15.4	15.3	15.1	15.0	14.9
	9.9	8.4	8.1	7.8	7.8	7.9	8.1	8.3	8.6	8.8	9.1
TS21. $C_2H_3 \rightarrow C_2H_2 + H$	39.6	39.8	39.9	40.2	40.3	40.3	40.2	40.1	39.9	39.6	39.4
	6.8	5.4	4.9	4.1	3.4	2.8	2.2	1.7	1.2	0.7	0.3
TS22. $C_2H_3 + CH_4 \rightarrow C_2H_4 + CH_3$	11.8	11.0	11.1	11.6	12.2	12.8	13.4	14.0	14.6	15.1	15.6
	19.5	18.5	18.5	18.7	19.1	19.6	20.1	20.6	21.1	21.6	22.1
TS23. $C_2H_3 + C_2H_6 \rightarrow C_2H_4 + C_2H_5$	10.0	9.5	9.7	10.2	10.8	11.4	12.0	12.6	13.1	13.7	14.2
	21.0	20.2	20.2	20.5	20.9	21.4	21.9	22.4	23.0	23.5	24.0
TS24. $C_2H_2 + H \rightarrow C_2H + H_2$	34.6	34.1	33.9	33.7	33.4	33.1	32.8	32.5	32.2	31.9	31.7
	2.8	2.0	2.1	2.1	2.3	2.5	2.7	2.9	3.1	3.4	3.6
TS25. $C_2H_6 + CH_3 \rightarrow C_2H_5 + CH_4$	14.3	13.5	13.5	13.9	14.4	15.0	15.6	16.2	16.7	17.3	17.8
	17.7	16.6	16.7	17.1	17.7	18.3	18.9	19.5	20.0	20.6	21.1
TS26. $C_2H_6 + {}^3CH_2 \rightarrow C_2H_5 + CH_3$	8.7	7.9	8.1	8.7	9.3	10.0	10.6	11.2	11.8	12.4	12.9
	17.6	16.4	16.3	16.5	17.0	17.5	18.0	18.6	19.1	19.7	20.2
TS27. $C_2H_4 + HCl \rightarrow C_2H_5Cl$	41.9	40.5	40.4	40.4	40.6	40.8	41.1	41.4	41.7	42.0	42.2
	58.2	58.3	58.4	58.6	58.6	58.6	58.5	58.3	58.1	57.9	57.6
TS28. $C_2H_2 + HCl \rightarrow C_2H_3Cl$	47.1	45.7	45.4	45.2	45.2	45.2	45.3	45.4	45.5	45.6	45.7
	72.2	72.6	72.9	73.3	73.5	73.5	73.5	73.4	73.2	73.0	72.8
TS29. $C_2H_5 + HCl \rightarrow C_2H_5Cl + H$	28.4	27.0	26.9	26.9	27.2	27.5	27.8	28.2	28.5	28.8	29.1
	9.7	8.8	8.7	8.6	8.4	8.3	8.1	7.9	7.7	7.6	7.4
TS30. $C_2H_5 + HCl \rightarrow C_2H_6 + Cl$	0.4	−1.0	−1.2	−1.2	−1.1	−0.8	−0.5	−0.2	0.1	0.4	0.7
	−1.9	−2.4	−2.3	−2.0	−1.8	−1.5	−1.4	−1.3	−1.3	−1.3	−1.3
TS31. $C_2H_3 + HCl \rightarrow C_2H_3Cl + H$	23.4	22.4	22.3	22.5	22.8	23.1	23.5	23.8	24.1	24.4	24.7
	15.7	14.9	14.8	14.5	14.2	13.9	13.6	13.4	13.1	12.9	12.6
TS32. $C_2H_3 + HCl \rightarrow C_2H_4 + Cl$	−1.0	−2.2	−2.3	−2.3	−2.0	−1.7	−1.4	−1.1	−0.8	−0.5	−0.2
	7.7	7.1	7.1	7.3	7.4	7.5	7.6	7.6	7.6	7.6	7.6
TS33. $^3CH_2 + HCl \rightarrow CH_3 + Cl$	0.0	−1.1	−1.1	−0.9	−0.6	−0.2	0.2	0.5	0.9	1.2	1.5
	6.6	5.9	5.9	6.1	6.4	6.6	6.7	6.8	6.8	6.8	6.8
TS34. $^3CH_2 + HCl \rightarrow CH_2Cl + H$	25.0	23.7	23.7	23.8	24.1	24.5	24.9	25.2	25.5	25.9	26.2
	14.4	13.4	13.3	13.1	12.9	12.7	12.6	12.4	12.2	12.0	11.8
TS35. $SiCl_2 + SiCl_4 \rightarrow Si_2Cl_6$	13.7	13.7	13.9	14.3	14.7	15.1	15.5	15.9	16.3	16.7	17.1
	46.4	46.2	46.0	45.7	45.4	45.0	44.7	44.3	43.9	43.5	43.1
TS36. $SiCl_4 + H_2 \rightarrow SiHCl_3 + HCl$	61.7	60.2	59.8	59.4	59.2	59.2	59.4	59.5	59.8	60.0	60.3
	44.7	44.0	43.9	44.0	44.3	44.5	44.8	45.1	45.4	45.7	46.0
TS37. $SiCl_3 + H_2 \rightarrow SiHCl_3 + H$	16.3	15.2	15.0	15.0	15.3	15.6	16.0	16.4	16.8	17.2	17.6
	3.6	2.9	2.8	2.7	2.6	2.6	2.5	2.4	2.3	2.1	2.0
TS38. $SiCl_3 + H_2 \rightarrow SiHCl_2 + HCl$	48.4	46.8	46.4	45.8	45.7	45.7	45.8	46.0	46.2	46.5	46.8
	30.2	29.3	29.2	29.2	29.3	29.6	29.9	30.2	30.5	30.7	31.0
TS39. $SiCl_3 + HCl \rightarrow SiCl_4 + H$	15.0	14.5	14.6	15.1	15.6	16.0	16.5	16.9	17.3	17.6	17.9
	19.2	18.5	18.3	18.1	17.9	17.7	17.5	17.3	17.1	16.9	16.7
TS40. $SiCl_3 + HCl \rightarrow SiHCl_3 + Cl$	8.8	7.8	7.7	7.7	7.9	8.2	8.5	8.7	9.0	9.3	9.6
	−2.5	−2.9	−3.0	−3.1	−3.2	−3.3	−3.4	−3.5	−3.6	−3.8	−3.9

TABLE 1 (Continued)

reaction	0 K	298.15 K	400 K	600 K	800 K	1000 K	1200 K	1400 K	1600 K	1800 K	2000 K
TS41. $SiCl_2 + H_2 \rightarrow SiH_2Cl_2$	40.4	38.6	38.2	37.8	37.7	37.7	37.9	38.1	38.4	38.7	38.9
	72.3	72.4	72.3	72.2	72.1	71.9	71.6	71.4	71.1	70.8	70.4
TS42. $SiCl_2 + H_2 \rightarrow SiHCl + HCl$	34.3	32.6	32.1	31.6	31.5	31.6	31.7	32.0	32.3	32.5	32.8
	4.6	3.3	3.1	3.0	3.2	3.5	3.8	4.1	4.4	4.7	4.9
TS43. $SiCl_2 + H_2 \rightarrow SiHCl_2 + H$	51.2	50.1	50.0	50.0	50.2	50.5	50.8	51.2	51.5	51.9	52.2
	−6.5	−7.1	−7.2	−7.4	−7.6	−7.7	−7.9	−8.1	−8.2	−8.4	−8.6
TS44. $SiCl_2 + HCl \rightarrow SiCl_3 + H$	33.3	32.8	33.0	33.4	33.9	34.4	34.8	35.2	35.6	36.0	36.3
	−6.2	−7.0	−7.1	−7.3	−7.5	−7.7	−8.0	−8.2	−8.4	−8.6	−8.8
TS45. $SiHCl_3 \rightarrow SiCl_2 + HCl$	67.1	67.4	67.4	67.3	67.1	66.9	66.6	66.3	66.0	65.7	65.4
	16.7	15.7	15.7	15.8	16.0	16.3	16.6	17.0	17.3	17.5	17.8
TS46. $SiH_2Cl_2 \rightarrow SiHCl + HCl$	68.7	68.9	69.0	68.9	68.8	68.6	68.4	68.2	67.9	67.6	67.3
	7.1	5.9	5.8	5.9	6.1	6.4	6.7	7.0	7.3	7.6	7.8
TS47. $SiHCl_3 + H_2 \rightarrow SiH_2Cl_2 + HCl$	62.3	60.8	60.4	60.0	59.8	59.8	59.9	60.1	60.3	60.6	60.9
	43.7	43.0	42.9	42.9	43.1	43.4	43.7	44.0	44.3	44.6	44.8
TS48. $SiHCl_2 + H_2 \rightarrow SiH_2Cl_2 + H$	16.8	15.6	15.5	15.5	15.7	16.0	16.4	16.8	17.2	17.6	18.0
	3.7	3.0	2.9	2.8	2.7	2.7	2.6	2.5	2.4	2.3	2.1
TS49. $SiHCl_2 + HCl \rightarrow SiHCl_3 + H$	14.8	14.2	14.3	14.7	15.2	15.6	16.0	16.4	16.8	17.1	17.5
	20.2	19.4	19.3	19.0	18.8	18.6	18.4	18.2	18.1	17.9	17.7
TS50. $SiHCl_2 + HCl \rightarrow SiH_2Cl_2 + Cl$	8.8	7.9	7.8	7.7	7.9	8.1	8.4	8.6	8.9	9.1	9.4
	−2.9	−3.2	−3.3	−3.4	−3.5	−3.7	−3.8	−3.9	−4.1	−4.2	−4.4
TS51. $SiHCl + H_2 \rightarrow SiH_3Cl$	19.0	17.2	16.8	16.4	16.2	16.2	16.4	16.6	16.8	17.0	17.3
	62.4	62.4	62.4	62.4	62.2	62.0	61.8	61.5	61.2	60.9	60.6
TS52. $SiHCl + HCl \rightarrow SiHCl_2 + H$	25.6	24.6	24.7	25.1	25.5	26.0	26.4	26.8	27.1	27.5	27.8
	−2.4	−3.3	−3.5	−3.7	−3.9	−4.1	−4.3	−4.5	−4.7	−4.9	−5.1
TS53. $SiCl_3 + CH_4 \rightarrow CH_3SiCl_3 + H$	40.3	39.8	40.0	40.7	41.5	42.3	43.0	43.6	44.3	44.8	45.4
	29.7	28.8	28.6	28.2	27.8	27.5	27.3	27.0	26.8	26.5	26.3
TS54. $SiCl_3 + CH_4 \rightarrow SiHCl_3 + CH_3$	18.3	18.1	18.4	19.3	20.1	20.9	21.7	22.4	23.0	23.6	24.2
	6.0	5.6	5.7	6.0	6.5	7.0	7.5	7.9	8.4	8.9	9.3
TS55. $SiCl_3 + CH_3 \rightarrow SiCl_2 + CH_3Cl$	0.6	0.0	0.1	0.3	0.6	1.0	1.4	1.8	2.2	2.6	3.0
	19.6	19.9	20.4	21.3	22.0	22.6	23.2	23.7	24.2	24.7	25.2
TS56. $SiCl_3 + CH_3 \rightarrow SiHCl_3 + {}^3CH_2$	20.6	20.2	20.5	21.1	21.8	22.6	23.2	23.9	24.5	25.1	25.7
	2.8	2.5	2.7	3.2	3.8	4.3	4.9	5.4	5.9	6.4	6.8
TS57. $SiCl_2 + CH_4 \rightarrow CH_3SiHCl_2$	64.0	63.0	63.1	63.5	64.1	64.7	65.3	65.9	66.4	67.0	67.5
	97.0	97.0	96.9	96.7	96.4	96.2	95.8	95.5	95.2	94.8	94.5
TS58. $CH_2SiCl_2 + H_2 \rightarrow CH_3SiHCl_2$	30.7	29.0	28.6	28.1	27.9	27.9	28.0	28.2	28.4	28.7	28.9
	89.9	89.9	90.0	90.0	90.0	89.9	89.8	89.6	89.4	89.2	88.9
TS59. $CH_3SiHCl_2 \rightarrow CH_2SiHCl + HCl$	78.6	78.6	78.7	78.9	78.9	79.0	78.9	78.8	78.6	78.4	78.2
	4.4	3.3	3.3	3.3	3.6	3.9	4.3	4.6	4.9	5.2	5.5
TS60. $CH_3SiCl_2 + H_2 \rightarrow CH_3SiHCl_2 + H$	16.0	14.8	14.7	14.7	14.9	15.3	15.6	16.1	16.5	16.8	17.2
	3.6	2.9	2.8	2.7	2.6	2.6	2.5	2.4	2.3	2.1	2.0
TS61. $CH_2SiCl_3 + H_2 \rightarrow CH_3SiCl_3 + H$	13.1	11.3	11.0	10.6	10.6	10.7	11.0	11.3	11.6	11.9	12.2
	11.4	10.5	10.3	10.2	10.2	10.1	10.1	10.0	10.0	9.9	9.8
TS62. $CH_3 + CH_3SiCl_3 \rightarrow CH_4 + CH_2SiCl_3$	12.6	11.8	11.8	12.2	12.7	13.2	13.8	14.4	14.9	15.5	16.0
	13.7	12.9	13.0	13.5	14.1	14.8	15.4	16.0	16.6	17.2	17.7
TS63. $CH_3 + CH_3SiCl_3 \rightarrow CH_3Cl + CH_3SiCl_2$	33.6	33.0	32.9	33.0	33.1	33.4	33.7	34.0	34.3	34.7	35.1
	5.9	6.2	6.5	7.1	7.7	8.2	8.6	9.1	9.5	9.9	10.4
TS64. $SiCl_3 + CH_3SiCl_3 \rightarrow SiHCl_3 + CH_2SiCl_3$	13.9	14.3	14.6	15.4	16.2	17.0	17.7	18.3	18.9	19.5	20.1
	2.8	2.9	3.0	3.5	4.0	4.5	5.0	5.5	6.0	6.5	7.0
TS65. $SiCl_3 + CH_3SiCl_3 \rightarrow SiCl_4 + CH_3SiCl_2$	17.7	18.3	18.6	19.1	19.6	20.0	20.4	20.8	21.2	21.6	22.0
	14.7	15.3	15.6	16.1	16.5	16.9	17.3	17.7	18.1	18.5	18.9
TS66. $H + CH_3SiCl_3 \rightarrow HCl + CH_3SiCl_2$	20.6	19.8	19.7	19.4	19.2	19.0	18.8	18.6	18.4	18.2	18.0
	13.4	12.8	12.9	13.3	13.8	14.3	14.7	15.1	15.5	15.8	16.1
TS67. $Cl + CH_3SiCl_3 \rightarrow HCl + CH_2SiCl_3$	3.2	2.9	3.0	3.3	3.6	3.8	4.0	4.0	4.1	4.1	4.0
	3.4	2.2	2.1	2.2	2.5	2.8	3.2	3.5	3.8	4.1	4.4
TS68. $CH_3SiCl_2 \rightarrow H + CH_2SiCl_2$	72.8	72.8	73.0	73.2	73.4	73.5	73.5	73.4	73.2	73.0	72.8
	1.2	−0.0	−0.3	−0.6	−1.0	−1.2	−1.5	−1.7	−1.9	−2.2	−2.4
TS69. $CH_3SiCl_3 \rightarrow CH_3SiCl_2Cl$	95.7	95.9	95.9	95.6	95.3	94.9	94.6	94.2	93.8	93.4	93.1
	−15.5	−15.6	−15.7	−16.1	−16.4	−16.8	−17.2	−17.5	−17.9	−18.3	−18.7
TS70. $CH_3SiCl_2Cl \rightarrow CH_3SiCl + Cl_2$	22.0	21.9	21.8	21.5	21.2	20.9	20.5	20.2	19.8	19.4	19.0
	4.8	4.4	4.5	4.6	4.8	5.0	5.1	5.3	5.5	5.7	5.9
TS71. $CH_3SiCl + H_2 \rightarrow CH_3SiH_2Cl$	24.9	22.9	22.5	22.0	21.7	21.7	21.9	22.1	22.3	22.5	22.8
	67.4	67.4	67.3	67.2	67.0	66.8	66.5	66.2	65.9	65.6	65.3
TS72. $CH_3SiCl + HCl \rightarrow CH_3SiHCl_2$	6.2	5.2	5.1	5.2	5.4	5.7	6.0	6.3	6.6	6.9	7.1
	69.0	69.3	69.3	69.2	69.1	68.9	68.7	68.5	68.2	67.9	67.5
TS73. $SiHCl_2 \rightarrow SiCl_2 + H$	44.9	45.6	45.8	46.0	46.1	46.0	45.9	45.7	45.4	45.1	44.8
	−0.2	−0.8	−0.9	−1.1	−1.3	−1.5	−1.7	−1.9	−2.1	−2.3	−2.5

[a] Classical energies are obtained at the estimated CCSD(T)/aug-cc-pVTZ//MP2/aug-cc-pVDZ level of theory. Zero point energies and partition functions are obtained at the MP2/aug-cc-pVDZ level of theory.

CH_3SiCl_3 can also undergo 1,2-elimination of HCl to produce CH_2SiCl_2. The HCl elimination reaction has the lowest free energy of activation, 81.0 kcal/mol, among all eight MTS molecular elimination reactions at 0 K. However, the $CH_3SiCl_3 \rightarrow CH_2SiCl_2 + HCl$ free energy of activation is 36.6 kcal/mol higher than that for $CH_3SiCl_3 \rightarrow CH_3 + SiCl_3$ at 1400 K. So, $CH_3SiCl_3 \rightarrow CH_2SiCl_2 + HCl$ is not the primary reaction at high temperatures, because it has a tight transition state structure and therefore is not favored by entropic effects at high temperatures.

The fifth decomposition reaction of MTS is a three-centered Cl-shift reaction, in which a Cl atom shifts from Si to C along with Si−C cleavage to form CH_3Cl and $^1SiCl_2$. This three-centered reaction has a 109.0 (100.9) kcal/mol forward free energy of activation at 0 (1400) K, higher than that for the HCl elimination reaction.

TABLE 2: Forward (Upper Entry) and Reverse (Lower Entry) Entropies of Activation (cal/(mol K)) at Various Temperatures Ranging from 0 to 2000 K[a]

reaction	0 K	298.15 K	400 K	600 K	800 K	1000 K	1200 K	1400 K	1600 K	1800 K	2000 K
TS1. $CH_3SiCl_3 \rightarrow CH_2SiCl_2 + HCl$	0.0	4.3	4.5	4.7	4.8	4.8	4.7	4.6	4.5	4.4	4.2
	0.0	−32.0	−32.2	−32.0	−31.6	−31.2	−30.9	−30.7	−30.5	−30.3	−30.1
TS2. $CH_3SiCl_3 \rightarrow CH_3Cl + SiCl_2$	0.0	6.7	6.6	6.2	5.8	5.5	5.1	4.8	4.6	4.3	4.1
	0.0	−33.4	−32.5	−31.2	−30.4	−29.9	−29.5	−29.1	−28.8	−28.6	−28.4
TS3. $Cl + H_2 \rightarrow HCl + H$	0.0	−18.6	−19.2	−19.7	−19.9	−19.9	−19.9	−19.9	−19.9	−19.9	−19.9
	0.0	−21.4	−22.0	−22.5	−22.7	−22.8	−22.9	−23.0	−23.1	−23.1	−23.2
TS4. $Cl + HCl \rightarrow Cl_2 + H$	0.0	−21.1	−21.4	−21.6	−21.7	−21.8	−22.0	−22.1	−22.2	−22.4	−22.5
	0.0	−19.2	−19.9	−20.8	−21.3	−21.8	−22.2	−22.5	−22.7	−23.0	−23.2
TS5. $CH_3 + H_2 \rightarrow CH_4 + H$	0.0	−25.6	−26.9	−27.8	−28.0	−27.9	−27.7	−27.5	−27.3	−27.2	−27.0
	0.0	−19.7	−20.2	−20.4	−20.4	−20.4	−20.4	−20.4	−20.4	−20.5	−20.5
TS6. $CH_3 + H \rightarrow {}^3CH_2 + H_2$	0.0	−20.4	−21.1	−21.6	−21.7	−21.8	−21.9	−22.0	−22.0	−22.1	−22.2
	0.0	−24.4	−25.2	−25.7	−25.7	−25.5	−25.3	−25.1	−24.9	−24.7	−24.5
TS7. $CH_3 + CH_3 \rightarrow {}^3CH_2 + CH_4$	0.0	−24.5	−24.8	−24.5	−23.9	−23.3	−22.8	−22.4	−22.0	−21.7	−21.4
	0.0	−22.5	−22.2	−21.1	−20.1	−19.4	−18.8	−18.3	−17.9	−17.6	−17.3
TS8. $CH_3 + HCl \rightarrow CH_3Cl + H$	0.0	−29.7	−30.3	−30.4	−30.2	−29.9	−29.6	−29.4	−29.2	−29.0	−28.8
	0.0	−21.8	−22.0	−22.3	−22.4	−22.6	−22.7	−22.8	−23.0	−23.1	−23.2
TS9. $CH_3 + HCl \rightarrow CH_4 + Cl$	0.0	−29.4	−30.0	−30.2	−29.9	−29.6	−29.3	−29.1	−28.9	−28.7	−28.6
	0.0	−20.6	−20.4	−19.8	−19.4	−19.1	−18.9	−18.9	−18.8	−18.8	−18.8
TS10. $CH_3Cl + H_2 \rightarrow CH_4 + HCl$	0.0	−20.7	−20.8	−20.7	−20.5	−20.3	−20.1	−19.9	−19.8	−19.6	−19.5
	0.0	−22.6	−22.3	−21.4	−20.6	−20.0	−19.6	−19.3	−19.0	−18.8	−18.7
TS11. $CH_2Cl + HCl \rightarrow CH_2Cl_2 + H$	0.0	−33.1	−33.5	−33.4	−33.0	−32.6	−32.3	−32.1	−31.9	−31.7	−31.5
	0.0	−20.5	−20.8	−21.2	−21.4	−21.6	−21.8	−21.9	−22.0	−22.1	−22.2
TS12. $C_2H_6 \rightarrow C_2H_4 + H_2$	0.0	2.1	2.2	2.4	2.6	2.7	2.7	2.7	2.6	2.5	2.5
	0.0	−27.1	−28.4	−29.6	−29.9	−29.9	−29.8	−29.6	−29.4	−29.3	−29.1
TS13. $C_2H_6(e) \rightarrow C_2H_4 + H_2$	0.0	3.4	4.2	5.5	6.3	6.9	7.3	7.6	7.8	7.9	8.1
	0.0	−25.8	−26.9	−27.8	−28.1	−28.0	−27.9	−27.7	−27.5	−27.4	−27.2
TS14. $C_2H_6 + H \rightarrow C_2H_5 + H_2$	0.0	−18.8	−19.2	−19.4	−19.4	−19.4	−19.5	−19.5	−19.5	−19.6	−19.6
	0.0	−29.1	−30.3	−31.2	−31.3	−31.2	−31.0	−30.8	−30.6	−30.4	−30.3
TS15. $C_2H_5 \rightarrow C_2H_4 + H$	0.0	−1.8	−1.9	−1.9	−2.0	−2.1	−2.2	−2.3	−2.5	−2.6	−2.8
	0.0	−20.8	−21.4	−22.2	−22.6	−22.9	−23.1	−23.3	−23.5	−23.6	−23.7
TS16. $C_2H_4 \rightarrow CH_2C + H_2$	0.0	5.1	6.0	7.1	7.6	7.9	7.9	7.9	7.8	7.7	7.6
	0.0	−27.2	−28.3	−29.1	−29.3	−29.3	−29.3	−29.2	−29.1	−29.0	−28.9
TS17. $CH_2C \rightarrow HCHC$	0.0	−0.1	−0.5	−1.2	−1.8	−2.2	−2.5	−2.8	−3.1	−3.3	−3.5
	0.0	−0.2	−0.6	−1.3	−1.9	−2.4	−2.8	−3.1	−3.4	−3.6	−3.8
TS18. $HCHC \rightarrow C_2H_2$	0.0	−0.4	−0.7	−1.2	−1.7	−2.1	−2.4	−2.7	−3.0	−3.2	−3.4
	0.0	4.2	3.5	2.5	1.8	1.2	0.7	0.4	0.0	−0.3	−0.6
TS19. $CH_3CH(s) \rightarrow C_2H_2 + H_2$	0.0	0.6	1.0	1.8	2.2	2.6	2.8	2.9	3.0	3.1	3.2
	0.0	−24.3	−26.3	−28.2	−29.1	−29.4	−29.6	−29.6	−29.6	−29.6	−29.6
TS20. $C_2H_4 + H \rightarrow C_2H_3 + H_2$	0.0	−19.3	−19.7	−20.1	−20.4	−20.5	−20.6	−20.7	−20.8	−20.9	−21.0
	0.0	−26.4	−27.2	−27.9	−27.9	−27.8	−27.6	−27.4	−27.3	−27.1	−27.0
TS21. $C_2H_3 \rightarrow C_2H_2 + H$	0.0	0.9	1.4	1.9	2.1	2.1	2.1	1.9	1.8	1.7	1.5
	0.0	−19.9	−21.4	−23.0	−24.0	−24.7	−25.2	−25.6	−25.9	−26.2	−26.5
TS22. $C_2H_3 + CH_4 \rightarrow C_2H_4 + CH_3$	0.0	−28.0	−27.6	−26.6	−25.8	−25.1	−24.5	−24.1	−23.7	−23.4	−23.1
	0.0	−26.8	−26.8	−26.4	−25.9	−25.3	−24.9	−24.5	−24.1	−23.8	−23.6
TS23. $C_2H_3 + C_2H_6 \rightarrow C_2H_4 + C_2H_5$	0.0	−30.2	−29.7	−28.7	−27.8	−27.1	−26.6	−26.1	−25.8	−25.5	−25.2
	0.0	−33.4	−33.3	−32.8	−32.2	−31.6	−31.1	−30.7	−30.4	−30.1	−29.8
TS24. $C_2H_2 + H \rightarrow C_2H + H_2$	0.0	−16.1	−16.5	−17.1	−17.5	−17.8	−18.1	−18.3	−18.5	−18.7	−18.8
	0.0	−20.0	−20.0	−19.9	−19.7	−19.5	−19.3	−19.1	−18.9	−18.8	−18.7
TS25. $C_2H_6 + CH_3 \rightarrow C_2H_5 + CH_4$	0.0	−24.4	−24.3	−23.6	−22.8	−22.2	−21.6	−21.2	−20.8	−20.5	−20.2
	0.0	−28.8	−28.6	−27.8	−27.0	−26.4	−25.8	−25.3	−25.0	−24.6	−24.4
TS26. $C_2H_6 + {}^3CH_2 \rightarrow C_2H_5 + CH_3$	0.0	−25.6	−25.1	−24.0	−23.1	−22.4	−21.8	−21.3	−20.9	−20.6	−20.3
	0.0	−31.9	−32.1	−31.7	−31.0	−30.5	−29.9	−29.5	−29.2	−28.8	−28.6
TS27. $C_2H_4 + HCl \rightarrow C_2H_5Cl$	0.0	−30.3	−30.7	−30.7	−30.4	−30.2	−29.9	−29.7	−29.5	−29.3	−29.2
	0.0	1.1	1.3	1.6	1.7	1.7	1.6	1.5	1.3	1.2	1.0
TS28. $C_2H_2 + HCl \rightarrow C_2H_3Cl$	0.0	−27.8	−28.6	−29.1	−29.1	−29.0	−28.9	−28.8	−28.8	−28.7	−28.7
	0.0	2.9	3.6	4.4	4.7	4.8	4.7	4.7	4.6	4.4	4.3
TS29. $C_2H_5 + HCl \rightarrow C_2H_5Cl + H$	0.0	−34.5	−34.9	−34.8	−34.4	−34.1	−33.8	−33.5	−33.3	−33.2	−33.0
	0.0	−22.1	−22.4	−22.7	−22.9	−23.1	−23.2	−23.4	−23.5	−23.6	−23.7
TS30. $C_2H_5 + HCl \rightarrow C_2H_6 + Cl$	0.0	−33.0	−33.6	−33.7	−33.5	−33.2	−32.9	−32.7	−32.5	−32.3	−32.1
	0.0	−20.0	−19.7	−19.1	−18.7	−18.4	−18.3	−18.2	−18.2	−18.2	−18.2
TS31. $C_2H_3 + HCl \rightarrow C_2H_3Cl + H$	0.0	−31.0	−31.1	−30.8	−30.4	−30.0	−29.7	−29.5	−29.3	−29.1	−28.9
	0.0	−21.2	−21.7	−22.3	−22.7	−23.1	−23.3	−23.5	−23.7	−23.8	−23.9
TS32. $C_2H_3 + HCl \rightarrow C_2H_4 + Cl$	0.0	−30.4	−30.7	−30.6	−30.3	−29.9	−29.7	−29.4	−29.2	−29.0	−28.9
	0.0	−20.5	−20.4	−20.1	−19.8	−19.7	−19.6	−19.6	−19.6	−19.6	−19.6
TS33. $^3CH_2 + HCl \rightarrow CH_3 + Cl$	0.0	−26.4	−26.5	−26.1	−25.6	−25.2	−24.9	−24.6	−24.4	−24.2	−24.0
	0.0	−19.6	−19.5	−19.1	−18.8	−18.6	−18.5	−18.4	−18.4	−18.4	−18.4
TS34. $^3CH_2 + HCl \rightarrow CH_2Cl + H$	0.0	−27.4	−27.5	−27.2	−26.7	−26.3	−26.0	−25.7	−25.5	−25.3	−25.2
	0.0	−23.2	−23.6	−24.0	−24.3	−24.5	−24.6	−24.8	−24.9	−25.0	−25.1
TS35. $SiCl_2 + SiCl_4 \rightarrow Si_2Cl_6$	0.0	−35.6	−35.0	−34.2	−33.6	−33.1	−32.8	−32.5	−32.2	−32.0	−31.8
	0.0	0.4	0.1	−0.5	−1.0	−1.4	−1.7	−2.0	−2.3	−2.5	−2.7
TS36. $SiCl_4 + H_2 \rightarrow SiHCl_3 + HCl$	0.0	−21.3	−22.3	−23.2	−23.5	−23.5	−23.4	−23.2	−23.1	−22.9	−22.8
	0.0	−30.4	−30.4	−30.2	−29.9	−29.6	−29.3	−29.1	−28.9	−28.7	−28.6
TS37. $SiCl_3 + H_2 \rightarrow SiHCl_3 + H$	0.0	−25.1	−25.5	−25.5	−25.2	−24.8	−24.5	−24.1	−23.9	−23.7	−23.5
	0.0	−20.0	−20.3	−20.5	−20.6	−20.7	−20.8	−20.9	−20.9	−21.0	−21.1
TS38. $SiCl_3 + H_2 \rightarrow SiHCl_2 + HCl$	0.0	−25.4	−26.6	−27.6	−27.9	−27.9	−27.8	−27.6	−27.5	−27.3	−27.2
	0.0	−33.1	−33.4	−33.4	−33.2	−32.9	−32.7	−32.4	−32.2	−32.1	−31.9
TS39. $SiCl_3 + HCl \rightarrow SiCl_4 + H$	0.0	−31.5	−31.1	−30.2	−29.5	−29.0	−28.5	−28.2	−28.0	−27.8	−27.6
	0.0	−17.3	−17.7	−18.2	−18.5	−18.7	−18.9	−19.1	−19.2	−19.3	−19.4
TS40. $SiCl_3 + HCl \rightarrow SiHCl_3 + Cl$	0.0	−30.2	−30.5	−30.5	−30.3	−30.0	−29.7	−29.5	−29.3	−29.2	−29.0
	0.0	−22.2	−22.4	−22.7	−22.8	−22.9	−23.0	−23.1	−23.2	−23.3	−23.4

TABLE 2 (Continued)

reaction	0 K	298.15 K	400 K	600 K	800 K	1000 K	1200 K	1400 K	1600 K	1800 K	2000 K
TS41. $SiCl_2 + H_2 \rightarrow SiH_2Cl_2$	0.0	−28.5	−29.6	−30.5	−30.6	−30.6	−30.4	−30.3	−30.1	−29.9	−29.8
	0.0	1.6	1.5	1.3	1.1	0.9	0.7	0.5	0.3	0.1	−0.1
TS42. $SiCl_2 + H_2 \rightarrow SiHCl + HCl$	0.0	−27.1	−28.3	−29.4	−29.6	−29.5	−29.4	−29.2	−29.0	−28.8	−28.7
	0.0	−33.1	−33.6	−33.8	−33.6	−33.3	−33.0	−32.8	−32.6	−32.4	−32.2
TS43. $SiCl_2 + H_2 \rightarrow SiHCl_2 + H$	0.0	−22.6	−22.9	−22.9	−22.7	−22.3	−22.0	−21.8	−21.5	−21.3	−21.1
	0.0	−22.2	−22.5	−22.9	−23.1	−23.3	−23.4	−23.6	−23.7	−23.8	−23.9
TS44. $SiCl_2 + HCl \rightarrow SiCl_3 + H$	0.0	−29.4	−29.0	−28.1	−27.4	−26.8	−26.4	−26.1	−25.9	−25.7	−25.5
	0.0	−21.4	−21.8	−22.2	−22.5	−22.8	−23.0	−23.1	−23.2	−23.4	−23.5
TS45. $SiHCl_3 \rightarrow SiCl_2 + HCl$	0.0	4.8	4.8	4.5	4.3	4.1	3.8	3.6	3.4	3.2	3.0
	0.0	−32.0	−32.2	−32.0	−31.6	−31.3	−31.0	−30.8	−30.6	−30.4	−30.3
TS46. $SiH_2Cl_2 \rightarrow SiHCl + HCl$	0.0	4.0	4.1	4.0	3.8	3.6	3.4	3.2	3.1	2.9	2.7
	0.0	−32.1	−32.3	−32.2	−31.9	−31.6	−31.3	−31.1	−30.9	−30.7	−30.6
TS47. $SiHCl_3 + H_2 \rightarrow SiH_2Cl_2 + HCl$	0.0	−24.4	−25.5	−26.5	−26.8	−26.8	−26.6	−26.5	−26.3	−26.2	−26.0
	0.0	−31.1	−31.3	−31.2	−30.9	−30.6	−30.4	−30.1	−29.9	−29.8	−29.6
TS48. $SiHCl_2 + H_2 \rightarrow SiH_2Cl_2 + H$	0.0	−25.1	−25.5	−25.6	−25.3	−24.9	−24.5	−24.2	−24.0	−23.7	−23.6
	0.0	−19.0	−19.3	−19.5	−19.6	−19.6	−19.7	−19.8	−19.8	−19.9	−20.0
TS49. $SiHCl_2 + HCl \rightarrow SiHCl_3 + H$	0.0	−31.1	−30.8	−29.9	−29.3	−28.8	−28.4	−28.1	−27.8	−27.6	−27.5
	0.0	−18.3	−18.7	−19.1	−19.4	−19.6	−19.8	−20.0	−20.1	−20.2	−20.3
TS50. $SiHCl_2 + HCl \rightarrow SiH_2Cl_2 + Cl$	0.0	−28.4	−28.7	−28.7	−28.5	−28.3	−28.1	−27.9	−27.7	−27.6	−27.4
	0.0	−19.4	−19.6	−19.8	−20.0	−20.1	−20.2	−20.3	−20.4	−20.5	−20.6
TS51. $SiHCl + H_2 \rightarrow SiH_3Cl$	0.0	−28.8	−30.0	−30.9	−31.1	−31.1	−31.0	−30.8	−30.7	−30.5	−30.4
	0.0	2.5	2.6	2.4	2.2	2.0	1.8	1.6	1.4	1.2	1.1
TS52. $SiHCl + HCl \rightarrow SiHCl_2 + H$	0.0	−31.7	−31.4	−30.7	−30.1	−29.6	−29.2	−28.9	−28.7	−28.5	−28.3
	0.0	−25.3	−25.8	−26.3	−26.6	−26.8	−27.0	−27.2	−27.3	−27.4	−27.5
TS53. $SiCl_3 + CH_4 \rightarrow CH_3SiCl_3 + H$	0.0	−30.4	−29.7	−28.2	−27.1	−26.3	−25.6	−25.1	−24.7	−24.4	−24.1
	0.0	−20.0	−20.7	−21.6	−22.1	−22.4	−22.7	−22.9	−23.0	−23.2	−23.3
TS54. $SiCl_3 + CH_4 \rightarrow SiHCl_3 + CH_3$	0.0	−23.5	−22.6	−20.9	−19.7	−18.7	−18.1	−17.5	−17.1	−16.8	−16.5
	0.0	−24.3	−24.1	−23.4	−22.7	−22.2	−21.7	−21.4	−21.1	−20.8	−20.5
TS55. $SiCl_3 + CH_3 \rightarrow SiCl_2 + CH_3Cl$	0.0	−27.8	−27.7	−27.2	−26.8	−26.4	−26.0	−25.7	−25.5	−25.2	−25.0
	0.0	−28.1	−26.7	−24.9	−23.8	−23.1	−22.6	−22.2	−21.9	−21.6	−21.4
TS56. $SiCl_3 + CH_3 \rightarrow SiHCl_3 + {}^3CH_2$	0.0	−24.1	−23.4	−22.1	−21.1	−20.3	−19.6	−19.1	−18.7	−18.4	−18.1
	0.0	−22.9	−22.3	−21.3	−20.4	−19.8	−19.3	−18.9	−18.6	−18.3	−18.1
TS57. $SiCl_2 + CH_4 \rightarrow CH_3SiHCl_2$	0.0	−32.5	−32.3	−31.4	−30.6	−29.9	−29.4	−28.9	−28.5	−28.2	−27.9
	0.0	0.7	0.5	0.0	−0.4	−0.7	−1.0	−1.2	−1.5	−1.7	−1.8
TS58. $CH_2SiCl_2 + H_2 \rightarrow CH_3SiHCl_2$	0.0	−27.5	−28.6	−29.7	−30.0	−30.0	−29.9	−29.8	−29.6	−29.5	−29.3
	0.0	0.0	0.1	0.2	0.2	0.1	−0.0	−0.1	−0.3	−0.4	−0.6
TS59. $CH_3SiHCl_2 \rightarrow CH_2SiHCl + HCl$	0.0	1.5	1.7	2.0	2.1	2.1	2.1	2.0	1.9	1.8	1.6
	0.0	−32.8	−33.0	−32.8	−32.5	−32.1	−31.8	−31.5	−31.3	−31.2	−31.0
TS60. $CH_3SiCl_2 + H_2 \rightarrow CH_3SiHCl_2 + H$	0.0	−25.0	−25.4	−25.5	−25.1	−24.8	−24.4	−24.1	−23.8	−23.6	−23.4
	0.0	−20.0	−20.3	−20.5	−20.6	−20.7	−20.8	−20.9	−20.9	−21.0	−21.1
TS61. $CH_2SiCl_3 + H_2 \rightarrow CH_3SiCl_3 + H$	0.0	−30.4	−31.5	−32.2	−32.2	−32.1	−31.9	−31.6	−31.4	−31.2	−31.1
	0.0	−20.2	−20.6	−20.8	−20.9	−20.9	−21.0	−21.0	−21.1	−21.1	−21.2
TS62. $CH_3 + CH_3SiCl_3 \rightarrow CH_4 + CH_2SiCl_3$	0.0	−27.4	−27.3	−26.6	−25.9	−25.3	−24.7	−24.3	−23.9	−23.6	−23.4
	0.0	−31.8	−31.5	−30.5	−29.6	−28.8	−28.3	−27.8	−27.4	−27.1	−26.8
TS63. $CH_3 + CH_3SiCl_3 \rightarrow CH_3Cl + CH_3SiCl_2$	0.0	−23.5	−23.8	−23.7	−23.5	−23.2	−23.0	−22.7	−22.5	−22.3	−22.1
	0.0	−29.5	−28.5	−27.2	−26.4	−25.9	−25.4	−25.1	−24.8	−24.5	−24.3
TS64. $SiCl_3 + CH_3SiCl_3 \rightarrow SiHCl_3 + CH_2SiCl_3$	0.0	−30.8	−29.8	−28.2	−27.0	−26.2	−25.5	−25.0	−24.6	−24.3	−24.0
	0.0	−35.9	−35.4	−34.5	−33.8	−33.2	−32.7	−32.3	−32.0	−31.7	−31.5
TS65. $SiCl_3 + CH_3SiCl_3 \rightarrow SiCl_4 + CH_3SiCl_2$	0.0	−22.7	−22.0	−21.0	−20.3	−19.8	−19.5	−19.1	−18.9	−18.6	−18.4
	0.0	−22.3	−21.5	−20.6	−20.0	−19.5	−19.2	−18.8	−18.6	−18.3	−18.1
TS66. $H + CH_3SiCl_3 \rightarrow HCl + CH_3SiCl_2$	0.0	−17.9	−18.3	−18.8	−19.1	−19.4	−19.6	−19.7	−19.9	−20.0	−20.1
	0.0	−31.7	−31.3	−30.5	−29.8	−29.3	−28.9	−28.6	−28.4	−28.2	−28.0
TS67. $Cl + CH_3SiCl_3 \rightarrow HCl + CH_2SiCl_3$	0.0	−21.9	−21.6	−21.0	−20.6	−20.4	−20.2	−20.2	−20.1	−20.1	−20.2
	0.0	−35.0	−35.4	−35.2	−34.8	−34.5	−34.1	−33.9	−33.7	−33.5	−33.3
TS68. $CH_3SiCl_2 \rightarrow H + CH_2SiCl_2$	0.0	−0.6	−0.2	0.4	0.6	0.7	0.7	0.6	0.5	0.4	0.3
	0.0	−23.1	−23.8	−24.6	−25.1	−25.4	−25.6	−25.8	−25.9	−26.1	−26.2
TS69. $CH_3SiCl_3 \rightarrow CH_3SiCl_2Cl$	0.0	7.2	7.0	6.5	6.1	5.7	5.3	5.1	4.8	4.6	4.4
	0.0	−0.8	−1.2	−1.9	−2.4	−2.8	−3.1	−3.4	−3.7	−3.9	−4.1
TS70. $CH_3SiCl_2Cl \rightarrow CH_3SiCl + Cl_2$	0.0	−1.5	−1.7	−2.2	−2.7	−3.0	−3.4	−3.6	−3.9	−4.1	−4.3
	0.0	−34.7	−34.4	−34.1	−33.9	−33.7	−33.5	−33.4	−33.2	−33.1	−33.0
TS71. $CH_3SiCl + H_2 \rightarrow CH_3SiH_2Cl$	0.0	−31.6	−32.9	−34.0	−34.3	−34.3	−34.2	−34.0	−33.9	−33.7	−33.6
	0.0	−0.3	−0.5	−0.7	−1.0	−1.2	−1.5	−1.7	−1.9	−2.1	−2.3
TS72. $CH_3SiCl + HCl \rightarrow CH_3SiHCl_2$	0.0	−33.3	−33.5	−33.4	−33.0	−32.7	−32.4	−32.2	−32.0	−31.8	−31.7
	0.0	3.9	3.9	3.8	3.7	3.5	3.3	3.1	2.9	2.7	2.5
TS73. $SiHCl_2 \rightarrow SiCl_2 + H$	0.0	5.6	6.2	6.7	6.7	6.7	6.5	6.4	6.2	6.1	5.9
	0.0	−18.3	−18.6	−19.0	−19.3	−19.5	−19.7	−19.9	−20.0	−20.1	−20.2

[a] Partition functions are obtained at the MP2/aug-cc-pVDZ level of theory.

The sixth and seventh MTS decomposition reactions produce the carbenes $^1CH_2$ and $^1CHSiCl_3$. The corresponding reverse reactions are high energy insertions of $^1CH_2$ into the Si−H bond of $SiHCl_3$ and $^1CHSiCl_3$ into H_2. Carbene insertion reactions are expected to have no or negligible energy barriers.[25−27] For example, Gordon and Gano found that $^1CH_2 + SiH_4 \rightarrow CH_3SiH_3$ and $^1CH_2 + CH_4 \rightarrow C_2H_6$ have no energy barrier at the MP3/6-31G(d)//HF/3-21G level of theory.[26] An MP2/aug-cc-pVDZ optimization starting from separate H_2 and $^1CHSiCl_3$ also shows that CH_3SiCl_3 can be formed without overcoming an energy barrier. Various optimization calculations starting from separate $^1CH_2$ and $SiHCl_3$ show that $^1CH_2$ tends to insert into a Si−Cl bond of $SiHCl_3$. One reason is that a Cl atom can donate one lone pair of electrons to the C of $^1CH_2$, which has the ability of accepting one pair of electrons with an empty valence orbital. $^1CH_2$ further forms a single bond with Si along with the Si−Cl bond cleavage. MP2/STO-3G level dynamic reaction coordinate calculations, however, suggest that $^1CH_2$ can insert into the Si−H bond of $SiHCl_3$, starting from separate $^1CH_2$ and $SiHCl_3$ with zero initial momentums. Therefore, it is reasonable to

TABLE 3: Forward (Upper Entry) and Reverse (Lower Entry) Free Energies of Activation (kcal/mol) at Various Temperatures Ranging from 0 to 2000 K[a]

reaction	0 K	298.15 K	400 K	600 K	800 K	1000 K	1200 K	1400 K	1600 K	1800 K	2000 K
TS1. $CH_3SiCl_3 \rightarrow CH_2SiCl_2 + HCl$	81.0	79.8	79.3	78.4	77.5	76.5	75.6	74.7	73.7	72.9	72.0
	2.2	10.8	14.0	20.5	26.8	33.1	39.3	45.5	51.6	57.7	63.7
TS2. $CH_3SiCl_3 \rightarrow CH_3Cl + SiCl_2$	109.0	107.3	106.6	105.3	104.1	103.0	101.9	100.9	100.0	99.1	98.3
	36.4	46.2	49.5	55.9	62.1	68.1	74.0	79.9	85.7	91.4	97.1
TS3. $Cl + H_2 \rightarrow HCl + H$	5.4	9.7	11.6	15.5	19.5	23.5	27.4	31.4	35.4	39.4	43.4
	3.8	9.0	11.3	15.7	20.2	24.8	29.4	34.0	38.6	43.2	47.8
TS4. $Cl + HCl \rightarrow Cl_2 + H$	47.8	53.4	55.6	59.9	64.2	68.5	72.9	77.3	81.8	86.2	90.7
	0.4	5.3	7.3	11.4	15.6	19.9	24.3	28.8	33.3	37.9	42.5
TS5. $CH_3 + H_2 \rightarrow CH_4 + H$	13.6	19.3	22.0	27.5	33.1	38.7	44.2	49.8	55.3	60.7	66.1
	13.1	17.8	19.8	23.9	28.0	32.0	36.1	40.2	44.3	48.4	52.5
TS6. $CH_3 + H \rightarrow {}^3CH_2 + H_2$	14.5	19.4	21.5	25.8	30.1	34.5	38.9	43.2	47.6	52.1	56.5
	9.5	15.1	17.6	22.7	27.9	33.0	38.1	43.1	48.1	53.0	58.0
TS7. $CH_3 + CH_3 \rightarrow {}^3CH_2 + CH_4$	16.8	22.8	25.3	30.3	35.1	39.8	44.4	48.9	53.4	57.7	62.0
	11.3	17.0	19.2	23.6	27.7	31.6	35.5	39.2	42.8	46.3	49.8
TS8. $CH_3 + HCl \rightarrow CH_3Cl + H$	30.6	38.0	41.1	47.2	53.2	59.2	65.2	71.1	76.9	82.7	88.5
	10.1	15.8	18.0	22.5	26.9	31.4	36.0	40.5	45.1	49.7	54.3
TS9. $CH_3 + HCl \rightarrow CH_4 + Cl$	2.3	9.5	12.5	18.5	24.5	30.5	36.4	42.2	48.0	53.8	59.5
	3.3	8.6	10.7	14.7	18.7	22.5	26.3	30.1	33.8	37.6	41.4
TS10. $CH_3Cl + H_2 \rightarrow CH_4 + HCl$	86.9	92.0	94.1	98.2	102.4	106.4	110.5	114.5	118.4	122.4	126.3
	107.0	112.7	115.0	119.3	123.5	127.6	131.5	135.4	139.3	143.1	146.8
TS11. $CH_2Cl + HCl \rightarrow CH_2Cl_2 + H$	33.2	41.8	45.2	51.8	58.5	65.0	71.5	78.0	84.4	90.7	97.0
	9.2	14.4	16.6	20.8	25.0	29.3	33.7	38.0	42.4	46.8	51.3
TS12. $C_2H_6 \rightarrow C_2H_4 + H_2$	122.9	122.2	122.0	121.6	121.1	120.5	120.0	119.5	118.9	118.4	117.9
	91.6	97.9	100.7	106.5	112.5	118.5	124.4	130.4	136.3	142.2	148.0
TS13. $C_2H_6(e) \rightarrow C_2H_4 + H_2$	113.5	112.7	112.4	111.4	110.2	108.9	107.4	105.9	104.4	102.8	101.2
	84.7	90.6	93.3	98.8	104.4	110.0	115.6	121.1	126.6	132.1	137.6
TS14. $C_2H_6 + H \rightarrow C_2H_5 + H_2$	10.2	14.8	16.7	20.6	24.5	28.4	32.3	36.2	40.1	44.0	47.9
	14.0	20.8	23.8	30.0	36.2	42.5	48.7	54.9	61.0	67.1	73.2
TS15. $C_2H_5 \rightarrow C_2H_4 + H$	38.9	39.2	39.4	39.8	40.2	40.6	41.0	41.5	41.9	42.5	43.0
	3.9	8.9	11.0	15.4	19.9	24.4	29.0	33.7	38.4	43.1	47.8
TS16. $C_2H_4 \rightarrow CH_2C + H_2$	92.6	91.4	90.9	89.6	88.1	86.5	84.9	83.4	81.8	80.2	78.7
	10.5	16.7	19.5	25.2	31.1	37.0	42.8	48.7	54.5	60.3	66.1
TS17. $CH_2C \rightarrow HCHC$	0.5	0.3	0.3	0.5	0.8	1.2	1.7	2.2	2.8	3.4	4.1
	−0.8	−0.9	−0.9	−0.7	−0.3	0.1	0.6	1.2	1.8	2.5	3.3
TS18. $HCHC \rightarrow C_2H_2$	0.1	0.1	0.2	0.4	0.6	1.0	1.5	2.0	2.5	3.2	3.8
	43.6	42.3	41.9	41.3	40.9	40.6	40.4	40.3	40.2	40.2	40.3
TS19. $CH_3CH(s) \rightarrow C_2H_2 + H_2$	33.2	33.2	33.2	32.9	32.5	32.0	31.4	30.9	30.3	29.7	29.0
	66.4	71.7	74.2	79.7	85.5	91.3	97.2	103.1	109.1	115.0	120.9
TS20. $C_2H_4 + H \rightarrow C_2H_3 + H_2$	17.1	21.9	23.9	27.9	32.0	36.0	40.2	44.3	48.4	52.6	56.8
	9.9	16.3	19.0	24.5	30.1	35.7	41.2	46.7	52.2	57.6	63.0
TS21. $C_2H_3 \rightarrow C_2H_2 + H$	39.6	39.5	39.4	39.0	38.6	38.2	37.8	37.4	37.0	36.7	36.3
	6.8	11.3	13.4	17.9	22.6	27.5	32.5	37.5	42.7	47.9	53.2
TS22. $C_2H_3 + CH_4 \rightarrow C_2H_4 + CH_3$	11.8	19.3	22.1	27.6	32.8	37.9	42.8	47.7	52.5	57.2	61.8
	19.5	26.5	29.2	34.5	39.8	44.9	49.9	54.8	59.7	64.5	69.2
TS23. $C_2H_3 + C_2H_6 \rightarrow C_2H_4 + C_2H_5$	10.0	18.5	21.6	27.4	33.1	38.6	43.9	49.2	54.4	59.5	64.6
	21.0	30.2	33.6	40.2	46.6	53.0	59.3	65.5	71.6	77.6	83.6
TS24. $C_2H_2 + H \rightarrow C_2H + H_2$	34.6	38.9	40.6	43.9	47.4	50.9	54.5	58.2	61.8	65.6	69.3
	2.8	8.0	10.1	14.1	18.0	21.9	25.8	29.6	33.4	37.2	41.0
TS25. $C_2H_6 + CH_3 \rightarrow C_2H_5 + CH_4$	14.3	20.8	23.2	28.0	32.7	37.2	41.5	45.8	50.0	54.1	58.2
	17.7	25.2	28.1	33.8	39.3	44.6	49.8	55.0	60.0	64.9	69.8
TS26. $C_2H_6 + {}^3CH_2 \rightarrow C_2H_5 + CH_3$	8.7	15.6	18.2	23.1	27.8	32.3	36.7	41.0	45.3	49.4	53.5
	17.6	25.9	29.1	35.5	41.8	47.9	54.0	59.9	65.8	71.6	77.3
TS27. $C_2H_4 + HCl \rightarrow C_2H_5Cl$	41.9	49.6	52.7	58.8	64.9	71.0	77.0	83.0	88.9	94.8	100.6
	58.2	58.0	57.9	57.6	57.3	56.9	56.6	56.3	56.0	55.8	55.5
TS28. $C_2H_2 + HCl \rightarrow C_2H_3Cl$	47.1	54.0	56.8	62.6	68.4	74.2	80.0	85.8	91.6	97.3	103.1
	72.2	71.8	71.4	70.6	69.7	68.8	67.8	66.9	66.0	65.1	64.2
TS29. $C_2H_5 + HCl \rightarrow C_2H_5Cl + H$	28.4	37.3	40.8	47.8	54.7	61.6	68.4	75.1	81.8	88.5	95.1
	9.7	15.4	17.7	22.2	26.8	31.4	36.0	40.7	45.4	50.1	54.8
TS30. $C_2H_5 + HCl \rightarrow C_2H_6 + Cl$	0.4	8.8	12.2	19.0	25.7	32.4	39.0	45.5	52.0	58.5	65.0
	−1.9	3.5	5.5	9.4	13.2	16.9	20.6	24.2	27.9	31.5	35.2
TS31. $C_2H_3 + HCl \rightarrow C_2H_3Cl + H$	23.4	31.6	34.8	41.0	47.1	53.1	59.1	65.0	70.9	76.7	82.5
	15.7	21.3	23.4	27.8	32.4	36.9	41.6	46.3	51.0	55.7	60.5
TS32. $C_2H_3 + HCl \rightarrow C_2H_4 + Cl$	−1.0	6.8	9.9	16.1	22.2	28.2	34.2	40.1	45.9	51.7	57.5
	7.7	13.2	15.2	19.3	23.3	27.2	31.1	35.1	39.0	42.9	46.8
TS33. $^3CH_2 + HCl \rightarrow CH_3 + Cl$	0.0	6.8	9.5	14.7	19.9	25.0	30.0	34.9	39.8	44.7	49.5
	6.6	11.8	13.7	17.6	21.4	25.1	28.8	32.5	36.2	39.9	43.5
TS34. $^3CH_2 + HCl \rightarrow CH_2Cl + H$	25.0	31.9	34.7	40.1	45.5	50.8	56.1	61.2	66.4	71.5	76.5
	14.4	20.3	22.7	27.5	32.3	37.2	42.1	47.0	52.0	57.0	62.0
TS35. $SiCl_2 + SiCl_4 \rightarrow Si_2Cl_6$	13.7	24.3	27.9	34.8	41.6	48.3	54.9	61.4	67.8	74.3	80.6
	46.4	46.0	46.0	46.0	46.2	46.4	46.8	47.1	47.6	48.1	48.6
TS36. $SiCl_4 + H_2 \rightarrow SiHCl_3 + HCl$	61.7	66.5	68.8	73.3	78.0	82.7	87.4	92.0	96.7	101.3	105.8
	44.7	53.0	56.1	62.2	68.2	74.1	80.0	85.9	91.7	97.4	103.2
TS37. $SiCl_3 + H_2 \rightarrow SiHCl_3 + H$	16.3	22.7	25.2	30.4	35.4	40.4	45.4	50.2	55.0	59.8	64.5
	3.6	8.9	10.9	15.0	19.1	23.3	27.4	31.6	35.8	40.0	44.2
TS38. $SiCl_3 + H_2 \rightarrow SiHCl_2 + HCl$	48.4	54.3	57.0	62.4	68.0	73.6	79.1	84.7	90.2	95.7	101.1
	30.2	39.2	42.5	49.2	55.9	62.5	69.1	75.6	82.0	88.5	94.9
TS39. $SiCl_3 + HCl \rightarrow SiCl_4 + H$	15.0	23.9	27.1	33.2	39.2	45.0	50.7	56.4	62.0	67.6	73.2
	19.2	23.6	25.4	29.0	32.7	36.4	40.2	44.0	47.8	51.6	55.5
TS40. $SiCl_3 + HCl \rightarrow SiHCl_3 + Cl$	8.8	16.9	19.9	26.1	32.1	38.2	44.1	50.1	56.0	61.8	67.6
	−2.5	3.7	6.0	10.5	15.1	19.7	24.3	28.9	33.5	38.2	42.8

TABLE 3 (Continued)

reaction	0 K	298.15 K	400 K	600 K	800 K	1000 K	1200 K	1400 K	1600 K	1800 K	2000 K
TS41. $SiCl_2 + H_2 \rightarrow SiH_2Cl_2$	40.4	47.1	50.1	56.1	62.2	68.3	74.4	80.5	86.5	92.5	98.5
	72.3	71.9	71.7	71.4	71.2	71.0	70.8	70.7	70.6	70.6	70.6
TS42. $SiCl_2 + H_2 \rightarrow SiHCl + HCl$	34.3	40.6	43.5	49.3	55.2	61.1	67.0	72.8	78.6	84.4	90.2
	4.6	13.2	16.6	23.3	30.0	36.7	43.4	49.9	56.5	63.0	69.4
TS43. $SiCl_2 + H_2 \rightarrow SiHCl_2 + H$	51.2	56.9	59.2	63.8	68.3	72.8	77.3	81.6	86.0	90.3	94.5
	−6.5	−0.5	1.8	6.3	10.9	15.6	20.3	25.0	29.7	34.4	39.2
TS44. $SiCl_2 + HCl \rightarrow SiCl_3 + H$	33.3	41.6	44.6	50.3	55.8	61.2	66.5	71.8	77.0	82.1	87.3
	−6.2	−0.6	1.6	6.0	10.5	15.0	19.6	24.2	28.8	33.5	38.2
TS45. $SiHCl_3 \rightarrow SiCl_2 + HCl$	67.1	65.9	65.5	64.5	63.6	62.8	62.0	61.3	60.6	59.9	59.3
	16.7	25.3	28.6	35.0	41.3	47.6	53.9	60.0	66.2	72.3	78.3
TS46. $SiH_2Cl_2 \rightarrow SiHCl + HCl$	68.7	67.7	67.3	66.5	65.7	65.0	64.3	63.6	63.0	62.4	61.8
	7.1	15.5	18.7	25.2	31.6	38.0	44.3	50.5	56.7	62.8	69.0
TS47. $SiHCl_3 + H_2 \rightarrow SiH_2Cl_2 + HCl$	62.3	68.1	70.6	75.8	81.2	86.5	91.9	97.2	102.5	107.7	112.9
	43.7	52.2	55.4	61.7	67.9	74.0	80.1	86.2	92.2	98.2	104.1
TS48. $SiHCl_2 + H_2 \rightarrow SiH_2Cl_2 + H$	16.8	23.1	25.7	30.8	35.9	40.9	45.9	50.7	55.6	60.3	65.1
	3.7	8.6	10.6	14.5	18.4	22.3	26.2	30.2	34.1	38.1	42.1
TS49. $SiHCl_2 + HCl \rightarrow SiHCl_3 + H$	14.8	23.4	26.6	32.7	38.6	44.4	50.1	55.8	61.3	66.9	72.4
	20.2	24.8	26.7	30.5	34.4	38.3	42.2	46.2	50.2	54.2	58.3
TS50. $SiHCl_2 + HCl \rightarrow SiH_2Cl_2 + Cl$	8.8	16.3	19.2	25.0	30.7	36.4	42.0	47.6	53.2	58.7	64.2
	−2.9	2.5	4.5	8.5	12.4	16.4	20.5	24.5	28.6	32.7	36.8
TS51. $SiHCl + H_2 \rightarrow SiH_3Cl$	19.0	25.8	28.8	34.9	41.1	47.3	53.5	59.7	65.9	72.0	78.1
	62.4	61.7	61.4	60.9	60.4	60.0	59.6	59.3	59.0	58.7	58.5
TS52. $SiHCl + HCl \rightarrow SiHCl_2 + H$	25.6	34.1	37.3	43.5	49.6	55.6	61.5	67.3	73.0	78.8	84.4
	−2.4	4.2	6.8	12.1	17.3	22.7	28.1	33.5	38.9	44.4	49.9
TS53. $SiCl_3 + CH_4 \rightarrow CH_3SiCl_3 + H$	40.3	48.8	51.9	57.7	63.2	68.5	73.7	78.8	83.8	88.7	93.5
	29.7	34.8	36.9	41.1	45.5	49.9	54.5	59.0	63.6	68.2	72.9
TS54. $SiCl_3 + CH_4 \rightarrow SiHCl_3 + CH_3$	18.3	25.1	27.5	31.8	35.9	39.7	43.4	46.9	50.4	53.8	57.1
	6.0	12.8	15.3	20.1	24.7	29.2	33.6	37.9	42.1	46.3	50.4
TS55. $SiCl_3 + CH_3 \rightarrow SiCl_2 + CH_3Cl$	0.6	8.3	11.2	16.6	22.0	27.4	32.6	37.8	42.9	48.0	53.0
	19.6	28.3	31.1	36.2	41.1	45.8	50.3	54.8	59.2	63.6	67.9
TS56. $SiCl_3 + CH_3 \rightarrow SiHCl_3 + {}^3CH_2$	20.6	27.4	29.8	34.4	38.7	42.8	46.8	50.7	54.5	58.2	61.8
	2.8	9.3	11.6	16.0	20.1	24.2	28.1	31.9	35.6	39.3	43.0
TS57. $SiCl_2 + CH_4 \rightarrow CH_3SiHCl_2$	64.0	72.7	76.0	82.4	88.6	94.6	100.5	106.4	112.1	117.8	123.4
	97.0	96.8	96.7	96.7	96.7	96.8	97.0	97.2	97.5	97.8	98.2
TS58. $CH_2SiCl_2 + H_2 \rightarrow CH_3SiHCl_2$	30.7	37.2	40.1	45.9	51.9	57.9	63.9	69.9	75.8	81.7	87.6
	89.9	89.9	89.9	89.9	89.8	89.8	89.8	89.8	89.9	89.9	90.0
TS59. $CH_3SiHCl_2 \rightarrow CH_2SiHCl + HCl$	78.6	78.2	78.0	77.7	77.3	76.8	76.4	76.0	75.6	75.2	74.9
	4.4	13.1	16.5	23.1	29.6	36.0	42.4	48.8	55.1	61.3	67.5
TS60. $CH_3SiCl_2 + H_2 \rightarrow CH_3SiHCl_2 + H$	16.0	22.3	24.9	30.0	35.0	40.0	44.9	49.8	54.6	59.3	64.0
	3.6	8.9	10.9	15.0	19.2	23.3	27.4	31.6	35.8	40.0	44.2
TS61. $CH_2SiCl_3 + H_2 \rightarrow CH_3SiCl_3 + H$	13.1	20.4	23.5	29.9	36.4	42.8	49.2	55.6	61.9	68.1	74.4
	11.4	16.5	18.6	22.7	26.9	31.1	35.2	39.4	43.6	47.9	52.1
TS62. $CH_3 + CH_3SiCl_3 \rightarrow CH_4 + CH_2SiCl_3$	12.6	20.0	22.7	28.1	33.4	38.5	43.5	48.4	53.2	58.0	62.7
	13.7	22.3	25.6	31.8	37.8	43.6	49.3	54.9	60.4	65.9	71.3
TS63. $CH_3 + CH_3SiCl_3 \rightarrow CH_3Cl + CH_3SiCl_2$	33.6	40.0	42.5	47.2	51.9	56.6	61.2	65.8	70.3	74.8	79.2
	5.9	14.9	17.9	23.4	28.8	34.0	39.2	44.2	49.2	54.1	59.0
TS64. $SiCl_3 + CH_3SiCl_3 \rightarrow SiHCl_3 + CH_2SiCl_3$	13.9	23.4	26.5	32.3	37.8	43.1	48.3	53.4	58.3	63.2	68.0
	2.8	13.6	17.2	24.2	31.0	37.7	44.3	50.8	57.3	63.6	70.0
TS65. $SiCl_3 + CH_3SiCl_3 \rightarrow SiCl_4 + CH_3SiCl_2$	17.7	25.1	27.4	31.7	35.8	39.8	43.7	47.6	51.4	55.2	58.9
	14.7	22.0	24.2	28.4	32.5	36.4	40.3	44.1	47.8	51.5	55.2
TS66. $H + CH_3SiCl_3 \rightarrow HCl + CH_3SiCl_2$	20.6	25.1	27.0	30.7	34.5	38.4	42.3	46.2	50.1	54.1	58.1
	13.4	22.2	25.5	31.6	37.7	43.6	49.4	55.1	60.8	66.5	72.1
TS67. $Cl + CH_3SiCl_3 \rightarrow HCl + CH_2SiCl_3$	3.2	9.4	11.7	15.9	20.1	24.2	28.2	32.3	36.3	40.3	44.4
	3.4	12.7	16.3	23.3	30.3	37.3	44.1	50.9	57.7	64.4	71.1
TS68. $CH_3SiCl_2 \rightarrow H + CH_2SiCl_2$	72.8	73.0	73.0	73.0	72.9	72.8	72.7	72.5	72.4	72.3	72.3
	1.2	6.9	9.3	14.1	19.1	24.2	29.3	34.4	39.6	44.8	50.0
TS69. $CH_3SiCl_3 \rightarrow CH_3SiCl_2Cl$	95.7	93.8	93.1	91.7	90.4	89.3	88.2	87.1	86.1	85.2	84.3
	−15.5	−15.4	−15.3	−14.9	−14.5	−14.0	−13.4	−12.8	−12.0	−11.3	−10.5
TS70. $CH_3SiCl_2Cl \rightarrow CH_3SiCl + Cl_2$	22.0	22.3	22.5	22.9	23.4	23.9	24.6	25.3	26.0	26.8	27.7
	4.8	14.7	18.2	25.1	31.9	38.6	45.3	52.0	58.7	65.3	71.9
TS71. $CH_3SiCl + H_2 \rightarrow CH_3SiH_2Cl$	24.9	32.3	35.6	42.3	49.2	56.0	62.9	69.7	76.5	83.2	90.0
	67.4	67.4	67.5	67.6	67.8	68.0	68.3	68.6	69.0	69.4	69.8
TS72. $CH_3SiCl + HCl \rightarrow CH_3SiHCl_2$	6.2	15.1	18.5	25.2	31.8	38.4	44.9	51.4	57.8	64.2	70.5
	69.0	68.1	67.7	66.9	66.2	65.5	64.8	64.2	63.6	63.0	62.5
TS73. $SiHCl_2 \rightarrow SiCl_2 + H$	44.9	43.9	43.3	42.0	40.7	39.3	38.0	36.7	35.5	34.2	33.0
	−0.2	4.7	6.5	10.3	14.1	18.0	22.0	25.9	29.9	33.9	38.0

[a] Classical energies are obtained at the estimated CCSD(T)/aug-cc-pVTZ//MP2/aug-cc-pVDZ level of theory. Zero point energies and partition functions are obtained at the MP2/aug-cc-pVDZ level of theory.

assume that the free energies of activation for these two reactions are close to the net reaction free energies.

An eighth decomposition pathway, $CH_3SiCl_3 \rightarrow CH_3SiCl + Cl_2$, is a two-step reaction at the MP2/aug-cc-pVDZ level of theory. CH_3SiCl_3 first undergoes an isomerization reaction to form CH_3SiCl_2Cl with a Si−Cl−Cl bridge, which is a local minimum at this level of theory. Then CH_3SiCl_2Cl can lose Cl_2 to form CH_3SiCl. However, dual level CCSD(T)/aug-cc-pVTZ//MP2/aug-cc-pVDZ calculations show that TS69, the transition state for $CH_3SiCl_3 \rightarrow CH_3SiCl_2Cl$, has a 15.5 kcal/mol lower free energy than CH_3SiCl_2Cl at 0 K. This suggests that CH_3SiCl_2Cl may not be a true local minimum. TS70, the transition state for $CH_3SiCl_2Cl \rightarrow CH_3SiCl + Cl_2$, lies 133.1 (125.2) kcal/mol above CH_3SiCl_3 at 0 (1400) K. $CH_3SiCl + Cl_2$ also lies 128.3 (73.1) kcal/mol above CH_3SiCl_3 at 0 (1400) K. So, it is likely that $CH_3SiCl_3 \rightarrow CH_3SiCl + Cl_2$ is negligible kinetically

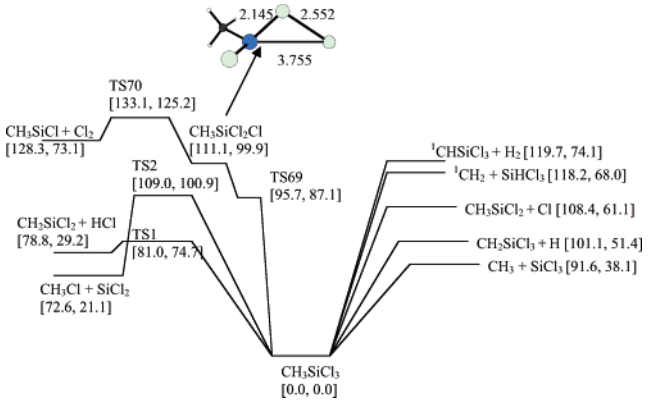

Figure 2. Unimolecular decomposition reaction pathways of CH_3SiCl_3. Numbers in square brackets are relative Gibbs free energies in kcal/mol at 0 K (left) and 1400 K (right), respectively.

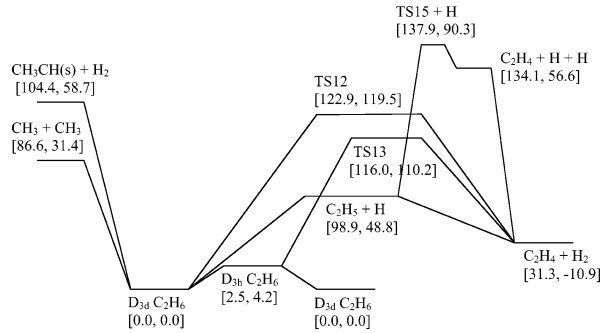

Figure 3. C_2H_6 potential energy surface. Numbers in square brackets are relative Gibbs free energies in kcal/mol at 0 K (left) and 1400 K (right), respectively.

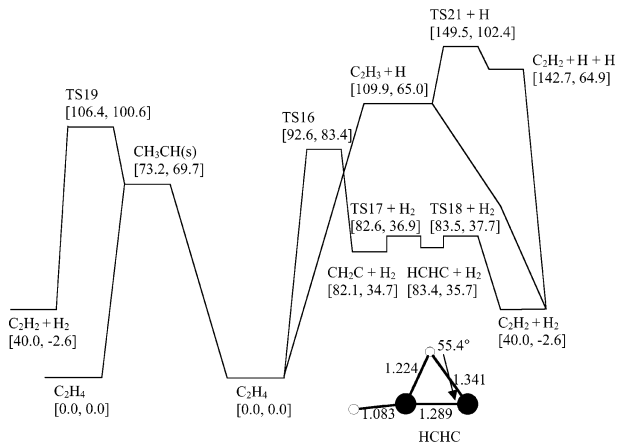

Figure 4. C_2H_4 potential energy surface. Numbers in square brackets are relative Gibbs free energies in kcal/mol at 0 K (left) and 1400 K (right), respectively.

and thermodynamically relative to the much more favored $CH_3SiCl_3 \rightarrow CH_3 + SiCl_3$ dissociation reaction at temperatures in the range 0−2000 K.

Overall, the 1,2-HCl elimination reaction is the predominant MTS decomposition reaction at low temperatures. However, at typical SiC CVD temperatures, such as 1400 K, Si−C bond cleavage of CH_3SiCl_3 becomes a competitive decomposition reaction pathway, followed by C−H and Si−Cl bond breaking reactions.

B. Potential Energy Surface of C_2H_6. C_2H_6 can be formed from the association reaction of two CH_3 radicals, where CH_3 can be produced from the Si−C bond cleavage of MTS. Because, as noted above, the latter reaction is important in the MTS CVD, it is possible that dehydrogenation of C_2H_6 might

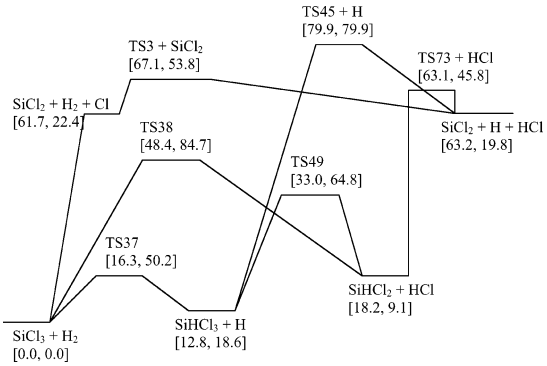

Figure 5. Potential energy surface of $[SiCl_3 + H_2]$. Numbers in square brackets are relative Gibbs free energies in kcal/mol at 0 K (left) and 1400 K (right), respectively.

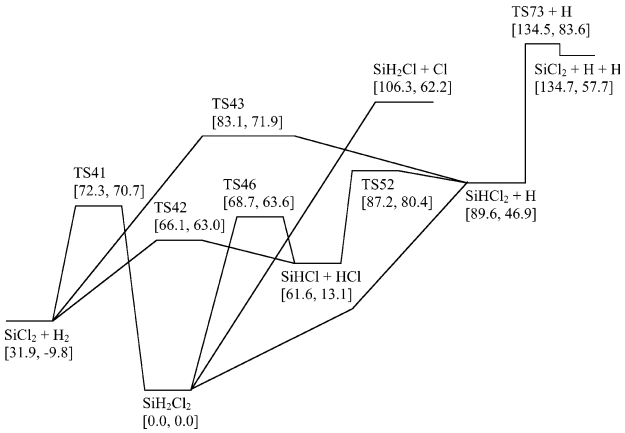

Figure 6. Potential energy surface of $[SiCl_2 + H_2]$. Numbers in square brackets are relative Gibbs free energies in kcal/mol at 0 K (left) and 1400 K (right), respectively.

be a major source of the production of C_2H_4 and C_2H_2 in the gas phase. Figure 3 illustrates the various pathways for the reaction $C_2H_6 \rightarrow C_2H_4 + H_2$. The negative relative free energies of $C_2H_4 + H_2$ at 1400 K is mainly due to the entropic effect. A C_s symmetry constrained C_2H_6(e) $\rightarrow C_2H_4 + H_2$ reaction path was discussed by Gordon, Truong, and Pople.[2] Herein, C_2H_6-(e) refers to eclipsed ethane and C_2H_6 refers to staggered ethane. A C_2 reaction path, starting from C_2H_6, has been found in this work. The forward barrier for $C_2H_6 \rightarrow C_2H_4 + H_2$ is 122.9 (119.5) kcal/mol at 0 (1400) K, higher than that of C_2H_6(e) $\rightarrow C_2H_4 + H_2$ (113.5, 105.9 kcal/mol at 0, 1400 K). A third pathway to C_2H_4 from C_2H_6 consists of two consecutive reaction steps: $C_2H_6 \rightarrow H + C_2H_5$ followed by $C_2H_5 \rightarrow H + C_2H_4$. $C_2H_6 \rightarrow H + C_2H_5$ has no transition state, whereas $C_2H_5 \rightarrow H + C_2H_4$ does have one (TS15). The predicted reverse activation free energy for $C_2H_5 \rightarrow H + C_2H_4$ is 3.9 kcal/mol at 0 K, agreeing well with the previous predictions by Hase et al.[7] (4.6 kcal/mol by QCISD(T)/6-311+G(2df,p) and 4.8 kcal/mol by MRCI/TZP+F).

Overall, the two unimolecular decomposition reaction paths through transition states TS12 and TS13 and the two-step reaction $C_2H_6 \rightarrow C_2H_5 + H \rightarrow C_2H_4 + H_2$ are the three major reaction paths for the production of C_2H_4 at low temperatures. The two-step reaction has a significantly lower free energy barrier than the unimolecular reactions at 1400 K due to the entropic effect; hence it may play the most important role in the production of C_2H_4 at CVD temperatures.

C. Potential Energy Surface of C_2H_4. The C_2H_4 PES presented in Figure 4 is similar to that in a previous study by Jensen, Morokuma, and Gordon,[3] suggesting two indirect

pathways that account for hydrogenation of C_2H_2, $C_2H_2 + H_2 \rightarrow CH_3CH(s) \rightarrow C_2H_4$ and $C_2H_2 + H_2 \rightarrow CH_2C + H_2 \rightarrow C_2H_4$. The $C_2H_2 + H_2 \rightarrow CH_3CH(s)$ reaction path is found to occur within C_s symmetry. $CH_3CH(s)$ has one imaginary frequency (450.5 cm^{-1}), that is, a transition state that leads to two identical ethylenes (C_2H_4). In the previous work by Jensen, Morokuma, and Gordon,[3] $CH_3CH(s)$ is a transition state that connects two identical CH_3CH molecules in C_1 symmetry ($CH_3CH(C_1)$). $CH_3CH(C_1)$ is slightly distorted from the C_s $CH_3CH(s)$ structure. Because the barrier that leads from CH_3CH to C_2H_4 is vanishingly small, and because the CH_3CH internal rotation barrier is also very small, the difference between the two sets of calculations is likely due to the higher levels of theory used in the present work and has no significant consequence. An HCHC intermediate with a C−H−C bridge (see Figure 4 for structural information) was located between CH_2C and C_2H_2. HCHC has no imaginary frequency at the MP2/aug-cc-pVDZ level of theory.

Transition states, TS17 and TS18, were located for the reactions $CH_2C \rightarrow HCHC$ and $HCHC \rightarrow C_2H_2$. The forward and reverse Gibbs activation free energies for $CH_2C \rightarrow HCHC$ are +0.5 and −0.8 kcal/mol at 0 K, respectively. This suggests that HCHC may not be a real local minimum. The forward and reverse Gibbs free energies of activation for $HCHC \rightarrow C_2H_2$ are 0.1 and 43.6 kcal/mol at 0 K. At 1400 K, the forward and reverse activation free energies for $CH_2C \rightarrow HCHC$ are 2.2 and 1.2 kcal/mol and those for $HCHC \rightarrow C_2H_2$ become 2.0 and 40.3 kcal/mol. Another $C_2H_4 \rightarrow C_2H_2 + H_2$ pathway involves two steps: $C_2H_4 \rightarrow C_2H_3 + H$ followed by $C_2H_3 + H \rightarrow C_2H_2 + H_2$. The first reaction has a 109.9 (65.0) kcal/mol forward free energy barrier at 0 (1400) K. The second (H abstraction) reaction is predicted to be barrierless.

No direct unimolecular decomposition reaction path has been found for $C_2H_4 \rightarrow C_2H_2 + H_2$ in the present work, in agreement with the previous study.[3] The lowest free energy reaction path for decomposition of C_2H_4 is $C_2H_4 \rightarrow CH_2C + H_2 \rightarrow C_2H_2 + H_2$ at 0 K. $C_2H_4 \rightarrow C_2H_3 + H \rightarrow C_2H_2 + H_2$ becomes one of the major pathways that accounts for the production of C_2H_2 at 1400 K due to entropic affects.

D. Potential Energy Surface of $SiCl_3 + H_2$. Figure 5 illustrates the $SiCl_3 + H_2$ potential energy surface. $SiCl_3$ radicals can be produced via an Si−C bond cleavage of MTS. H_2 often maintains a high and nearly constant concentration during the CVD of MTS for two possible reasons. One is that the overall MTS → SiC + 3HCl reaction neither produces nor consumes H_2. Second, H_2 is often the major component of the feeding gas in SiC CVD. There are two reaction pathways that involve both $SiCl_3$ and H_2 as reactants. The reaction $SiCl_3 + H_2 \rightarrow SiHCl_3 + H$ proceeds with a 16.3 (50.2) kcal/mol forward free energy of activation at 0 (1400 K). The reaction $SiCl_3 + H_2 \rightarrow SiHCl_2 + HCl$ proceeds with a 48.4 (84.7) kcal/mol forward free energy of activation at 0 (1400) K. The first of these reactions involves a three-center transition state, TS37, and the second involves a four-center transition state TS38. H can abstract a Cl atom from $SiHCl_3$ with a 20.2 (46.2) kcal/mol forward activation free energy at 0 (1400) K. The reverse activation energy is 14.8 (55.7) kcal/mol at 0 (1400) K. The $SiHCl_3 \rightarrow SiCl_2 + HCl$ transition state, TS45, has a high forward free energy of activation, 67.1 kcal/mol at 0 K and 61.3 kcal/mol at 1400 K. The reverse activation free energy is 16.7 (60.1) kcal/mol at 0 (1400) K. This suggests that both directions are slow at high CVD temperatures.

Bond breaking reactions are also illustrated in Figure 5. $SiCl_3$ may undergo a Si−Cl cleavage to produce $SiCl_2$. $SiHCl_2$ and $SiHCl_3$ may also break Si−H and/or Si−Cl bonds to produce SiHCl, $SiCl_2$, $SiHCl_2$, and/or $SiCl_3$. Bond breaking reactions are more likely to occur at 1400 K than at 0 K. For example, $SiCl_3 \rightarrow SiCl_2 + Cl$ has a 61.7 kcal/mol forward free energy requirement at 0 K that decreases to 22.4 kcal/mol barrier at 1400 K.

A transition state, TS73, was found for the $SiHCl_2 \rightarrow SiCl_2 + H$ bond-cleavage reaction. The forward activation free energy is 44.9 (36.7) kcal/mol at 0 (1400) K. The reverse activation free energy is a negligible −0.2 kcal/mol at 0 K that increases to 25.9 kcal/mol at 1400 K due to entropic affects.

Overall, $SiCl_3 + H_2 \rightarrow SiHCl_3 + H$ is the major reaction in this PES at low temperatures. Si−Cl cleavage of $SiCl_3$ becomes the predominant reaction at high CVD temperatures due to the entropic effect. $SiCl_3 \rightarrow SiCl_2 + Cl$ is expected to be one of the major sources for the production of $SiCl_2$ in the gas phase of SiC CVD.

E. Potential Energy Surface of $SiCl_2 + H_2$. Figure 6 illustrates the SiH_2Cl_2 PES. The $SiH_2Cl_2 \rightarrow SiCl_2 + H_2$ reaction has a high forward activation free energy of 72.3 (70.7) kcal/mol at 0 (1400 K). It is interesting to note that the molecular decomposition $SiH_2Cl_2 \rightarrow SiCl_2 + H_2$ is 31.9 kcal/mol endoergic at 0 K but becomes 9.8 kcal/mol *exo*ergic at 1400 K. However, the corresponding silylene insertion free energy of activation is 80.5 kcal/mol at 1400 K, so this process may be negligible at high CVD temperatures. The forward reaction free energy for $SiH_2Cl_2 \rightarrow SiHCl + HCl$ is 61.6 kcal/mol at 0 K and 13.1 kcal/mol at 1400 K, with corresponding activation free energies of 68.7 and 63.6, respectively. The reverse activation free energies are 7.1 and 50.5 kcal/mol. SiH_2Cl_2 requires 89.6 (46.9) kcal/mol to break a Si−H bond at 0 (1400) K.

A SiH_2Cl_2 Si−Cl bond cleavage requires 106.3 (62.2) kcal/mol at 0 (1400) K. H may abstract either a H or a Cl atom from $SiHCl_2$. The reaction $H + SiHCl_2 \rightarrow SiCl_2 + H_2$ has a negative activation free energy, after ZPE and higher order correlation corrections are included, at 0 K. The activation free energy becomes 25.0 kcal/mol at 1400 K. The reaction $SiHCl_2 + H \rightarrow SiHCl + HCl$ also has a negative activation free energy of −2.4 kcal/mol at 0 K that increases to 33.5 kcal/mol at 1400 K.

Overall, there are 2 competing reaction pathways for producing SiH_2Cl_2 from $SiCl_2$ and H_2. One is the direct $SiCl_2 + H_2 \rightarrow SiH_2Cl_2$ pathway through TS41. The other is a two-step reaction $SiCl_2 + H_2 \rightarrow SiHCl + HCl \rightarrow SiH_2Cl_2$ through transition states TS42 and TS46, respectively. The two-step reaction has 3.6 (7.1) kcal/mol lower overall free energy barrier than $SiCl_2 + H_2 \rightarrow SiH_2Cl_2$ at 0 (1400) K. Because both reaction pathways have high free energy barriers (>70 kcal/mol) at 1400 K, SiH_2Cl_2 is not expected to be a major component in the gas phase of SiC CVD process. This prediction is consistent with the experiments of Mousavipour et al.[28] and Zhang et al.[29]

IV. Conclusions

Reaction paths of 73 reactions with well-defined transition states that take place during and after the decomposition of MTS were studied. Structures, energies, and zero point energies of all transition states were calculated using the MP2 method. Higher level correlation energies were obtained at the CCSD(T) level of theory. Partition functions were also obtained using the MP2/aug-cc-pVDZ method to compute the thermodynamic contribution to enthalpies and entropies at 11 various temperatures from 0 to 2000 K. Potential energy surfaces of CH_3SiCl_3, C_2H_6, C_2H_4, $SiCl_3 + H_2$, and $SiCl_2 + H_2$ are illustrated at 0 and 1400 K. Activation enthalpy, entropy, and Gibbs free energy

obtained in this work are expected to be useful for future work on predicting rate constants for the various gas-phase reactions during and after the decomposition of methyltrichlorosilane. This work also sheds light on the gas-phase chemistry of CVD that involves C−H, C−H−Cl, C−H−Si, Si−Cl, and other different C−H−Si−Cl molecular systems.

Despite the authors' efforts to select significant gas-phase reactions, it is still difficult to predict a small set of key elementary reactions that have nontrivial effects on the SiC CVD process. In a subsequent work, accurate rate constants of the studied reactions will be obtained by transition state theory (TST), variational transition state theory (VTST) via the POLYRATE code,[30] RRKM theory via the RRKM code,[31] and molecular dynamics simulation via the VENUS code[32] using the geometric, energetic, and thermodynamic data presented in this and the preceding paper. This will facilitate the narrowing of the reaction set on a sound basis and will be addressed in subsequent papers. Surface reactions that may be involved in the SiC CVD process will also be investigated. More comprehensive kinetic simulations that include both gas-phase and surface reactions and take into account the heat transfer and mass transfer would eventually provide a reaction set that best simulates the reality.

Acknowledgment. This project is supported by the U.S. Department of Energy, Grant No. DE-FC07-05ID14661. Computer time was provided by the Scalable Computing Laboratory, Iowa State University. The authors are grateful to Drs. Mike Schmidt and Hui Li for valuable discussions.

Supporting Information Available: Tables of MP2 and CCSD(T) energies and zero point energies, Cartesian coordinates, and vibrational frequencies of all of the transition states studied in this work. This material is available free of charge via the Internet at http://pubs.acs.org.

References and Notes

(1) Ge, Y.; Gordon, M. S.; Battaglia, F.; Fox, R. O. *J. Phys. Chem.* **2007**, *111*, 1462.
(2) Gordon, M. S.; Truong, T. N.; Pople, J. A. *Chem. Phys. Letters* **1986**, *130*, 245.
(3) Jensen, J. H.; Morokuma, K.; Gordon, M. S. *J. Chem. Phys.* **1994**, *100*, 1981.
(4) Osterheld, T. H.; Allendorf, M. D.; Melius, C. F. *J. Phys. Chem.* **1994**, *98*, 6995.
(5) Allendorf, M. D.; Melius, C. F. *J. Phys. Chem.* **1993**, *97*, 720.
(6) Diau, E. W.; Lin, M. C.; Melius, C. F. *J. Chem. Phys.* **1994**, *101*, 3923.
(7) Hase, W. L.; Schlegel, H. B.; Balbyshev, V.; Page, M. *J. Phys. Chem.* **1996**, *100*, 5354.
(8) Hanninglee, M. A.; Green, N. J. B.; Pilling, M. J.; Robertson, S. H. *J. Phys. Chem.* **1993**, *97*, 860.
(9) Simon, Y.; Foucaut, J. F.; Scacchi, G. *Can. J. Chem.-Rev. Can. Chim.* **1988**, *66*, 2142.
(10) Trenwith, A. B. *J. Chem. Soc., Faraday Trans. 2* **1986**, *82*, 457.
(11) Loucks, L. F.; Laidler, K. J. *Can. J. Chem.* **1967**, *45*, 2795.
(12) Lin, M. C.; Back, M. H. *Can. J. Chem.* **1966**, *44*, 2357.
(13) Liu, G. X.; Li, Z. S.; Xiao, J. F.; Liu, J. Y.; Fu, Q.; Huang, X. R.; Sun, C. C.; Tang, A. C. *Chem. Phys. Chem.* **2002**, *3*, 625.
(14) Wu, T.; Werner, H. J.; Manthe, U. *Science* **2004**, *306*, 2227.
(15) Wittbrodt, J. M.; Schlegel, H. B. *Chem. Phys. Lett.* **1997**, *269*, 391.
(16) Walch, S. P.; Dateo, C. E. *J. Phys. Chem. A* **2001**, *105*, 2015.
(17) Walch, S. P.; Dateo, C. E. *J. Phys. Chem. A* **2002**, *106*, 2931.
(18) Aikens, C. M.; Webb, S. P.; Bell, R. L.; Fletcher, G. D.; Schmidt, M. W.; Gordon, M. S. *Theor. Chem. Acc.* **2003**, *110*, 233.
(19) Woon, D. E.; Dunning, T. H. *J. Chem. Phys.* **1993**, *98*, 1358.
(20) Dunning, T. H. *J. Chem. Phys.* **1989**, *90*, 1007.
(21) Schmidt, M. W.; Baldridge, K. K.; Boatz, J. A.; Elbert, S. T.; Gordon, M. S.; Jensen, J. H.; Koseki, S.; Matsunaga, N.; Nguyen, K. A.; Su, S. J.; Windus, T. L.; Dupuis, M.; Montgomery, J. A. *J. Comput. Chem.* **1993**, *14*, 1347.
(22) ACES II is a program product of the Quantum Theory Project, University of Florida. Authors: J. F. Stanton, J. Gauss, J. D. Watts, M. Nooijen, N. Oliphant, S. A. Perera, P. G. Szalay, W. J. Lauderdale, S. A. Kucharski, S. R. Gwaltney, S. Beck, A. Balková D. E. Bernholdt, K. K. Baeck, P. Rozyczko, H. Sekino, C. Hober, and R. J. Bartlett. Integral packages included are VMOL (J. Almlöf and P. R. Taylor); VPROPS (P. Taylor) ABACUS; (T. Helgaker, H. J. Aa. Jensen, P. Jørgensen, J. Olsen, and P. R. Taylor).
(23) Bode, B. M.; Gordon, M. S. *J. Mol. Graphics Model.* **1998**, *16*, 133.
(24) Allendorf, M. D.; Kee, R. J. *J. Electrochem. Soc.* **1991**, *138*, 841.
(25) Gordon, M. S.; Boatz, J. A.; Gano, D. R.; Friederichs, M. G. *J. Am. Chem. Soc.* **1987**, *109*, 1323.
(26) Gordon, M. S.; Gano, D. R. *J. Am. Chem. Soc.* **1984**, *106*, 5421.
(27) Sironi, M.; Cooper, D. L.; Gerratt, J.; Raimondi, M. *J. Am. Chem. Soc.* **1990**, *112*, 5054.
(28) Mousavipour, S. H.; Saheb, V.; Ramezani, S. *J. Phys. Chem. A* **2004**, *108*, 1946.
(29) Zhang, W. G. G.; Huttinger, K. J. *Chem. Vap. Deposition* **2001**, *7*, 173.
(30) Corchado, J. C.; Chuang, Y.-Y.; Fast, P. L.; Hu, W.-P.; Liu, Y.-P.; Lynch, G. C.; Nguyen, K. A.; Jackels, C. F.; Ramos, A. F.; Ellingson, B. A.; Lynch, B. J.; Melissas, V. S.; Villà, J.; Rossi, I.; Coitino, E. L.; Pu, J.; Albu, T. V.; Garrett, B. C.; Isaacson, A. D.; Truhlar, D. G. POLYRATE 9.4.3: Computer Program for the Calculation of Chemical Reaction Rates for Polyatomics, 2006.
(31) Zhu, L.; Hase, W. L. RRKM: A General RRKM Program, 1993.
(32) Hase, W. L.; Song, K.; Bolton, K.; de Sainte Claire, P.; Duchovic, R. J.; Hu, X.; Komornicki, A.; Li, G.; Lim, K. F.; Lu, D-h.; Peslherbe, G. H.; Mazyar, O. A.; Swamy, K. N.; Vande Linde, S. R.; Varandas, A.; Wang, H.; Wolf, R. J. VENUS05: A General Chemical Dynamics Computer Program, 2005.